

Chapter 1

An Observational Guide to Identifying Pseudobulges and Classical Bulges in Disk Galaxies

David B Fisher and Niv Drory

Abstract In this review our aim is to summarize the observed properties of pseudobulges and classical bulges. We utilize an empirical approach to studying the properties of bulges in disk galaxies, and restrict our analysis to statistical properties. A clear bimodality is observed in a number of properties including morphology, structural properties, star formation, gas content & stellar population, and kinematics. We conclude by summarizing those properties that isolate pseudobulges from classical bulges. Our intention is to describe a practical, easy to use, list of criteria for identifying bulge types.

1.1 Introduction

This paper reviews those observed properties of bulges that reveal the bimodal nature of the central structures found in disk galaxies. Our aim is to collect a set of empirical properties of bulges that can be used to diagnose bulges into the two sub-categories commonly referred to as *pseudobulges* and *classical bulges*. Despite a long history of studying bulges in disk galaxies (Sandage, 1961), and the knowledge that bulges are very common, being found in upwards of $\sim 80\%$ of bright galaxies ($> 10^9 M_{\odot}$; Fisher & Drory, 2011), only recently have systematic studies of the bimodal nature of bulges become frequent in the literature.

Kormendy & Illingworth (1983) have shown that bulges in disk galaxies separate by internal kinematics: some rotate rapidly like a disk where others are dominated by random motions (Kormendy & Illingworth, 1982). Also, the review by Wyse et al. (1997, and references therein) demonstrates clearly that bulges are a heterogeneous class of objects. Bulges are shown to vary significantly in their ages and metallic-

David B. Fisher
Swinburne University of Technology, e-mail: dfisher@swin.edu.au

Niv Drory
University of Texas, e-mail: drory@astro.as.utexas.edu

ities, and not all bulges show properties that are similar to elliptical galaxies. The observation that there is more than one type of bulge introduces the possibility that bulges as a class could be the end result of more than one mechanism of galaxy evolution.

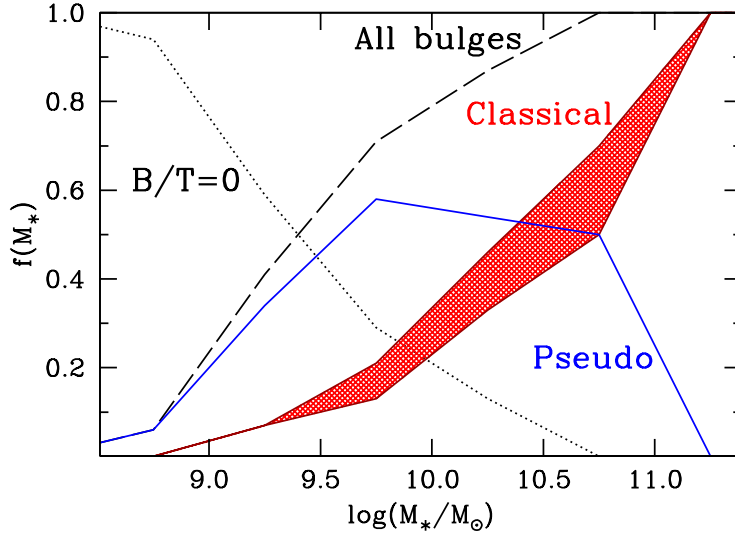


Fig. 1.1 The frequency of bulge types correlates with total galaxy mass. The four curves indicate the frequency of pseudobulges (blue solid line), classical bulges (red filled region), galaxies with no bulge (dotted line) and all bulges (dashed line) as a function of total galaxy mass. The classical bulges are shown as a shaded region because an attempt has been made to account for composite pseudobulge-classical systems. The higher value for a given mass includes this estimate, the lower value is for galaxies whose bulges are pure-classical bulge systems. There is a clear sequence of bulgeless galaxies existing at low mass, pseudobulges in intermediate mass galaxies and classical bulges in high mass galaxies.

In Fig. 1.1 we show a result that illustrates simple evidence that bulge type is connected to the evolution of galaxies. The figure shows the frequency of bulge types for the brightest ~ 100 galaxies in the local 11 Mpc volume. The type of bulge a galaxy contains changes systematically as galaxy mass increases. Similarly, galaxies with blue, young, stellar populations have been shown to have very different bulges than those of red, old galaxies (Drory & Fisher, 2007). These results suggest that bulge type is connected to the phenomena that drive galaxy evolution. Being able to diagnose bulge types in galaxies is therefore both useful to understand the properties of an individual galaxy, and also to understand galaxy evolution in general.

At present, we know of three main mechanisms that allow a galaxy to grow bulge mass (as measured by an increase in the bulge-to-total luminosity ratio from bulge-disk decompositions). These are merging processes (Hammer et al., 2005; Aguерri et al., 2001), slow secular evolution (Kormendy & Kennicutt, 2004;

Athanassoula, 2005a), and rapid internal evolution due to disk instabilities during the “clumpy” phase (Elmegreen et al., 2008; Inoue & Saitoh, 2012). It is therefore critical that we be able to identify the properties of bulges that potentially isolate features associated with each of these formation channels. Given that realistically the end result of bulge formation and evolution is likely a composite object, recognizing “pure” examples of each formation channel (i.e. the most extreme cases along a spectrum of properties) will be necessary to disentangle the physical processes involved.

In this review we will concentrate on work separating bulges into the dimorphic classes mentioned above. These two categories have been given names, the most popular of which seem to be “pseudobulges” and “classical bulges”. In short, pseudobulges are bulges that have properties that historically we associate with dissipative phenomena (active star formation, rotating kinematics, young stars; alternatively, some authors refer to such bulges as “disky bulges” (Athanassoula, 2005a)). Kormendy & Kennicutt (2004) give a thorough review, though now 10 years old, of pseudobulge properties. That review focuses largely on exemplary cases, while the review here will focus on statistical results, which can be applied to large sets of galaxies. “Classical bulges”, in turn, are those bulges that exhibit properties resembling elliptical galaxies, such as smooth distribution of stars, old stellar age, and kinematics dominated by random motions. The term “classical” refers to this being the widespread preconception about bulges for much of the 20th century (Wyse et al., 1997). Using a terminology that is based on preconceptions that are no longer widely held seems a bit archaic. Nonetheless, we accept the concept in language signification (known as *Saussurean Arbitrariness*), in which historic meaning or sound of a word is not as important as the meaning we ascribe to it now, and simply adopt the most popular terms of the present day (“pseudobulges” and “classical bulges”). For further reading on bulge properties we refer the reader to the aforementioned reviews by Kormendy & Kennicutt (2004) and Wyse et al. (1997), and also the lecture notes by Gadotti (2012) and Kormendy (2013).

1.1.1 Definition of a Bulge

Before discussing the separate kinds of bulges, it is necessary to define what is meant by the term “bulge” when applied to galaxies. The most commonly used definition of bulges is based on the observed rise in surface brightness above the disk that is observed at the center of many intermediate-type galaxies. Disk components of galaxies are often well described by an exponential decay with increasing radius of their surface brightness (Freeman, 1970). Many galaxy’s contain a centrally located structure that is brighter than the inward extrapolation of the disk’s exponential surface brightness, and this component is not associated with a bar. This central structure is often identified as a “bulge”. Bulges of this type are often identified using bulge-disk decomposition techniques (Kormendy, 1977b), commonly using the Sérsic function (Sérsic, 1968) to describe the surface brightness of the bulge. Defin-

ing bulges using surface photometry has the advantage that it is straightforward, empirically based, and can be applied to large numbers of galaxies. In principle one can use large data sets like the Sloan Digital Sky Survey to characterize bulges in $> 10^4$ galaxies (Lackner & Gunn, 2012).

Identifying bulges in bulge-disk decomposition is by nature parametric, but disk galaxies could have non-exponential components in their centers (similar to bars). Therefore, identifying extra light as a separate component may be misleading and physically meaningless. An alternate view of this is that in some intermediate-type galaxies, the bulge-disk decomposition simply reflects an empirical description of the surface brightness profile of star light. Another weakness of this method is that bulge-disk decomposition using the Sérsic function (described below) appears deceptively simple, yet the procedure carries with it a high degree of degeneracy.

Bulges are also identified as a 3-dimensional structure that “bulges” from the disk plane in the z direction. These structures are most easily identified in edge-on galaxies where bulging central structures are observed in the vast majority of massive galaxies (Kautsch et al., 2006). A significant caveat, however, to studying bulges in edge-on systems is that dust extinction from the disk significantly affects the light of the bulge, especially in galaxies with smaller bulges. Secondly, boxy bulges (Bureau & Freeman, 1999) which are the result of bars (Athanasoula, 2005b) can complicate the interpretation of bulge thickness. Two edge-on galaxies could have equally thick centers one with a boxy-bulge the other with a round thick bulge, which would be missed by blanket thickness cuts.

Kinematics can be used to identify a low-angular momentum and higher z -dispersion structure at the center of a high angular momentum thin disk. For example Fabricius et al. (2014) show that kinematics of the intermediate-type galaxy NGC 7217 clearly separates into two components one with high dispersion (the bulge) and the second with low dispersion (the disk). These components are consistent with a photometric bulge-disk decomposition. Ideally such procedure could be carried out on large numbers of galaxies in forthcoming data releases of SAMI (Croom et al., 2012) and MaNGA (Bundy et al., 2014). However, its not clear that either survey has sufficient spatial or spectral resolution to apply this technique.

1.1.2 Outline

Kormendy & Kennicutt’s (2004) review and Athanasoula (2005) make a strong case that multiple types of bulges exist, and that this is likely reflecting different channels of bulge formation and galaxy evolution. In this review, we discuss the identification of bulges of different types, attempting to provide practical means of classifying bulges.

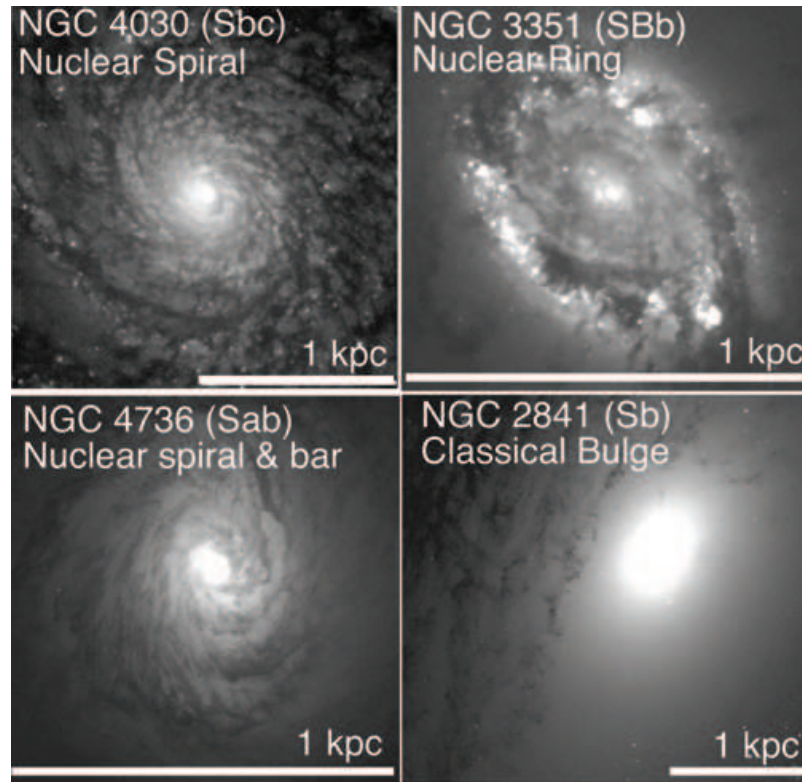


Fig. 1.2 Examples of bulge morphologies are shown using optical images from HST. The detectors and filters are NGC 4030: PC F606W; NGC 3351: PC F606W; NGC4736: PC F555W; and NGC 2841: ACS/WFC F435W. The white line in each panel represents 1 kpc. There is an extreme difference in these galaxies between pseudobulge morphologies (nuclear ring, spiral and bar) and classical bulges. In cases such as this, morphological diagnosis of bulge types is relatively straightforward.

1.2 Identifying Pseudobulges with Morphology

There are multiple lines of reasoning that motivate the morphological distinction of different bulge types. First, empirically speaking, results from *Hubble Space Telescope* (HST) imaging surveys are quite clear that there is not one single type of morphology that can be associated with regions of galaxies dominated by bulge light. This is in contrast to the description of bulges given in the *Carnegie Atlas of Galaxies* (Sandage & Bedke, 1994), in which bulges are described as having no evidence of a disk or “pure E” morphology. The presence of spiral structure (see, for example, Fig. 1.2) is in stark contrast to this definition. If the structure exhibiting the spiral, ring, or bar pattern is dominating the light then the classifier can be fairly confident that the dynamical state of the system better reflects that of disk kinemat-

ics than that of an elliptical galaxy. Morphology is therefore a physically motivated classification. However, we have to remind the reader of the problem in identifying such a disky structure as a distinct component as opposed to just being the physical state of the central disk.

From a certain point of view the simplest means of identifying bulges of different types is morphology. The main requirement is sufficient spatial resolution to identify small-scale features. Data from HST has made this a very straightforward process in which high quality identification of features like spiral structure can be done on nearby galaxies (< 50 Mpc). Typically, in this practice the user identifies, by-eye, features that are associated with disk morphology (such as spirals, rings, and bars) inside the region where the bulge dominates the light of the galaxy. Systematic studies comparing morphological bulge classification at different wavelengths would be useful. It stands to reason that broadband photometry at wavelengths in the middle of the optical spectrum (ie. V to I) are best suited. If the filter is too blue, the light becomes too sensitive to dust effects. Although, it has been shown that the morphological features identifying pseudobulges are present in near-IR images (Fisher & Drory, 2010), these features become difficult to see at longer wavelengths (eg. JHK bands).

Results from HST reveal that the centers of relatively “early type” galaxies (Sa-Sb) frequently contained spiral structure and show little evidence of a smooth featureless bulge (Carollo et al., 1997). In Fig. 1.2, top left panel, we show an example of nuclear spiral morphology. In this example, NGC 4030, the spiral is face-on and quite easy to identify. When present, the spiral structure frequently extends throughout the entire bulge, and reaches to the very center of the bulge region. In the centers of later type galaxies, such dusty spiral and non-smooth morphology becomes much more common than smooth, round bulges (Böker et al., 2002). In very nearby galaxies, e.g. NGC 5055, the presence of spiral structure that extends all the way to galaxy centers was recognized as early as 1961 in the Hubble Atlas (Sandage, 1961). Buta & Crocker (1993) identify a sample of nuclear spirals which they call pseudorings, placing first estimates on sizes (typical diameters of ~ 1 kpc). The advent of surveys from HST make it clear that nuclear spirals are very common in Sa-Sm galaxies (Fisher & Drory, 2011). Fisher & Drory (2008) introduce a secondary category of spirals referred to as nuclear patchy spirals. These are almost exclusively found in later type (Sc-Sd) galaxies with very small bulges.

A “nuclear ring” is a ring of stars and/or intense star formation found in the central region (radius < 1 kpc) of a disk galaxy (Buta & Crocker, 1993; Buta et al., 2007). Nuclear rings are often relatively easy to identify, and they are typically very bright due to their large star formation rates. Nuclear rings are separate from “inner rings” that are commonly found at the end of bars (de Vaucouleurs et al., 1991). Nuclear rings occur in roughly 20% of spiral galaxies (Knapen, 2005). Galaxies with nuclear rings are very likely to be barred (Comerón et al., 2010; Knapen, 2005). In Fig. 1.2 we show an example of a prominent nuclear ring in the nearby disk galaxy NGC 3351. Buta & Crocker (1993) identify galaxies with both nuclear rings and “pseudo-rings”. A pseudo-ring is when the ring is not fully formed, and does not

extend 360 degrees around the galaxy center. In fact, it may commonly refer to nuclear spirals.

Studies focusing on barred spirals find that secondary (nested) bars are frequent (Erwin & Sparke, 2002; Erwin et al., 2004). As many as 40% of S0-Sa galaxies with bars contain a secondary bar, extending to radii of 0.2-0.8 kpc. Many of the studies on secondary bars focus on early-type galaxies where there is less dust and the bars are easier to identify. Secondary bars in later-type galaxies are easily obscured by dust, and often hard to identify for that reason. Even in unobscured galaxies, it is useful to over-plot isophote contours of the galaxy to identify nuclear bars (as outlined by Erwin & Sparke 2002, also Erwin 2004). In Fig. 1.2 (bottom left panel) we show a galaxy with both a nuclear spiral and a nuclear bar. The bar is aligned north-to-south in the image. A number of simulations focus on the formation of galaxies with nested bars (Heller et al., 2007; Debattista & Shen, 2007; Shen & Debattista, 2009). These simulations generally find that the nuclear bars are rapidly rotating structures that form easily within barred disks.

Classical bulges are morphologically identified, in the ideal case, as having smooth centrally peaking isophotes that do not show any evidence of disk-like structure such as those described above. In Fig. 1.2 we show NGC 2841 as an example. In the image the smooth classical bulge is seen in the center, and at larger radii the effects from the disk become apparent. The presence of some extinction, indicating dust and gas, does not preclude a system from being a classical bulge; however in classical bulges when defined by morphology, such dust is not a dominant feature, nor is it embedded in a spiral pattern.

There are a number of caveats associated with morphological classification of bulge types. Using morphology as a means of identifying physically distinct phenomena is an inherently biased process by the person doing the identification. Two individuals can come to different conclusions about what is or is not a spiral pattern, or just a wisp of dust. Even with HST data, morphological classification is only possible at very low redshifts $z < 0.05$. Finally, in the absence of Galaxy Zoo type of analysis (e.g. Lintott et al., 2011) morphology is not a quantitative science; this limits both our ability to interpret the meaning and also to apply such analysis to large samples of objects.

Combining all disk-like structures (nuclear rings, nuclear spirals, and nuclear bars) into a single category of “pseudobulges” makes the assumption that these objects are linked. The conditions under which nuclear rings form are likely different than that of a secondary bar, nonetheless, the unifying concept is that all three are structures that are associated with disks. Furthermore, there is no significant differences between the bulge Sérsic index, bulge-to-total ratio or half-light radius of bulges with these structures (Fisher & Drory, 2008). The strongest difference appears to be between classical bulges and the rest of bulge morphologies.

In spite of the many caveats, morphological identification of bulge types seems quite useful. Bulges identified as pseudobulges using morphology are more actively forming stars (Fisher, 2006), have more disk-like kinematics (Fabricius et al., 2012), and occupy a different location in structural parameter space (Fisher & Drory, 2010) than classical bulges. These correlations will be discussed in more detail in subse-

quent sections, since their existence does establish that by-eye classification can accurately mark important distinctions.

1.3 Structural Properties of Bulges: Sérsic index, Scaling Relations, and Shape of Bulges

Structural parameters returned from bulge-disk decompositions can be a very powerful means to identify pseudobulges. In theory, bulge-disk decomposition software can be run on very large numbers of galaxies. If one can robustly identify bulge-types from the properties in decompositions alone, it is then straightforward to generate strong constraints on the number of bulges of each type in different environments. In practice, this procedure is complicated by inherent degeneracies in the decomposition procedure.

The process of bulge-disk decomposition assumes that the radial surface brightness profile, $I(r)$, of a galaxy can be described by a linear combination of a small number of component structures, such that $I(r) = I_{\text{bulge}}(r) + I_{\text{disk}}(r) + I_{\text{other}}(r)$, where I_{bulge} and I_{disk} describe the bulge and disk, and I_{other} describes any other structure in a galaxy.

There are a few systematic sources of uncertainty that should be taken into account to derive accurate parameters from bulge-disk decompositions. First, a well-known problem is accounting for galaxy structures that are neither bulge nor an exponential disk. Most commonly I_{other} describes light from a bar, but could also refer to rings, nuclei, or bright star forming spiral arms. Not taking a bar into account when modeling the light profile leads to systematic effects, such as overestimating the bulge-to-total ratio (B/T) by as much as a factor of two, and also systematically overestimating the value of the Sérsic index (Gadotti, 2008; Fisher & Drory, 2008; Laurikainen et al., 2006). If the galaxy has a central point source, either AGN or nucleus, this must be accounted for as well or else the returned model will have an artificially large Sérsic index and B/T .

Resolution is a crucial parameter for determining accurate Sérsic model parameters of bulge-disk decompositions. If the bulge is of the size of the resolution element, information on the size (half-light radius) and shape (Sérsic index) are completely untrustworthy (Gadotti, 2008; Fisher & Drory, 2008). Gadotti (2008) suggests that at least 80% of the half-light radius must be resolved. Fisher & Drory (2010) find that in order to determine accurate Sérsic indices of galaxies with small B/T , a resolution of 100 pc is preferred.

1.3.1 Using Sérsic Index to Identify Bulge Types

Typically, bulge-disk galaxies are decomposed using the Sérsic function (Sérsic, 1968) to describe the bulge. In this model the radial light profile in units of

mag arcsec⁻² of a galaxy can be described as

$$\mu_{\text{bulge}} = \mu(r_e) + b_n \left[\left(\frac{r}{r_e} \right)^{1/n_b} - 1 \right], \quad (1.1)$$

where n_b is the Sérsic index of the bulge; r represents radius, r_e is the radius containing half the light of the bulge, $\mu(r_e)$ is the surface brightness at r_e , and $b_n = 2.17n_b - 0.355$. The above formula, known as the Sérsic function (Sérsic, 1968), has been shown by a number of authors to describe the shape of elliptical galaxy profiles quite well (Caon et al., 1994). The case of a Sérsic function with $n_b = 1$ is equivalent to an exponential, commonly used to describe disks. The case of $n_b = 4$ is equivalent to the de Vaucouleurs profile used historically for E-type galaxies. There are a number of detailed discussions of the Sérsic function and its properties; for further reading see Graham & Driver (2005).

The Sérsic index of bulges is now widely used as a means to identify bulges, based largely on its correlation with other bulge properties (e.g. Fisher & Drory, 2008). The first evidence came from early surveys of bulge-disk decomposition in which it was clear that many bulges are better fit by double exponential profiles than by a traditional de Vaucouleurs profile (Andredakis & Sanders, 1994; Courteau et al., 1996). This was eventually generalized to show that all bulges are better described using the Sérsic function (Andredakis et al., 1995), and that later-type galaxies tend to have lower values of n_b . Results using HST images find that bulges with disk morphology are more likely to have shallow, more like exponential, surface brightness profiles (Scarlata et al., 2004).

Using ~ 100 galaxies with HST imaging, Fisher & Drory (2008) compare the morphology of bulges to the associated bulge Sérsic index from detailed bulge-disk decompositions. They find that there is a clear bimodal distribution of Sérsic indices in galaxies. To reduce uncertainty in the Sérsic index, the authors created composite surface photometry using HST data to measure the surface brightness profile of the inner 10 arcsec, and a set of deep wide-field images to measure the surface brightness profile of the outer parts of the galaxy (a similar procedure is discussed in Balcells et al., 2003 and Kormendy et al. (2009)). The result is a surface brightness profile that covers a very large dynamic range in radius, and is thus able to reduce uncertainty in Sérsic index, and better break the degeneracy between n and r_e (Graham et al., 1996). These decompositions reveal that 90% of bulges with morphology that indicates a pseudobulge (as described in the previous section) have $n_b < 2$, and all classical bulges and elliptical galaxies have $n_b > 2$. The authors followed up on this result with a larger sample of galaxies with near-IR photometry (still combining HST and in this case Spitzer IRAC 3.6 μm ; Fisher & Drory, 2010). The result is the same, all classical bulges are found to have $n_b > 2$ and over 90% of pseudobulges have $n_b < 2$.

To double check the correlation of bulge Sérsic index with high resolution bulge morphology we compile a sample of 308 galaxies that have both published bulge-disk decomposition and also have data in the HST archive from which we can determine the morphology of the bulge. The sources of n_b are Fisher & Drory (2008,

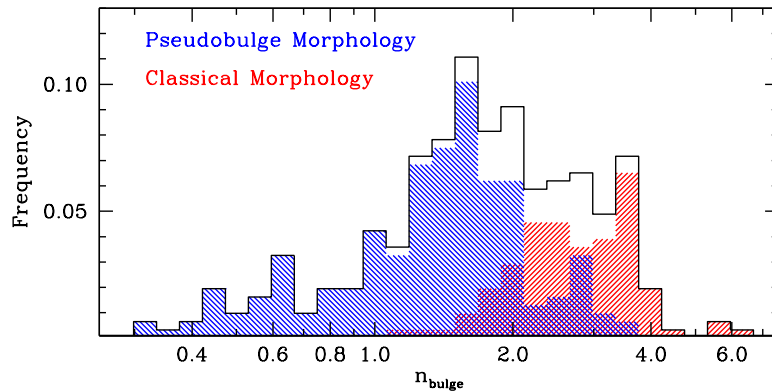


Fig. 1.3 The distribution of bulges Sérsic indices from a sample of 308 nearby bulge-disk galaxies with both published bulge-disk decompositions and available data in the HST archive for bulge morphology diagnosis. The distribution of n_{bulge} in galaxies with classical bulge morphology shown to be clearly different than that of pseudobulges.

2010, 2011); Fabricius et al. (2012); Fisher et al. (2013); Laurikainen et al. (2010); Weinzirl et al. (2009). In the case of overlapping galaxies we take the result that is based on the finest spatial resolution, though typically the spread in Sérsic index is not large, $\Delta n_b < 0.2$. In a few galaxies (~ 10) the spread in n_b is large, $\Delta n_b > 1$. We drop these galaxies assuming that the Sérsic index is poorly constrained and not trustworthy. The total sample combines decompositions from three independent fitting procedures (described in Fisher & Drory, 2008; Weinzirl et al., 2009; Laurikainen et al., 2010), and contains 106 S0-S0/a, 71 Sa-ab, 62 Sb-bc, 61 Sc-cd, 10 Sd-dm galaxies.

In Fig. 1.3 we show the distribution of Sérsic indices in the combined sample. There is a clear correlation between bulge type and Sérsic index. The choice of $n_b = 2$ as the dividing line is not arbitrary, but rather is justified by the coincidence of this value with the turnover in the two distributions. This is clearly evident in the figure. The sample contains 102 classical bulges and 87% of those classical bulges have $n_b > 2$, conversely in the sample we identify 205 galaxies as having pseudobulges and 86% of these have $n_b < 2$. If we consider only those galaxies with Hubble type Sa and later, the frequency of classical bulges with $n_b < 2$ drops to 7%, and the frequency of pseudobulges with larger Sérsic index ($n_b > 2$) becomes only slightly lower, 11%. We note that although not completely devoid of gas, S0 galaxies have significantly less dust and gas (Young et al., 2011), therefore identifying features such as nuclear spirals is much more difficult in these galaxies.

In addition, if we restrict the sample to only those galaxies where the resolution is better than 300 pc, the correlation becomes stronger. In the improved-resolution sample, we find that only 6% of the classical bulges have low Sérsic index and roughly 9% of pseudobulges have high Sérsic index. If we exclude both S0 galaxies

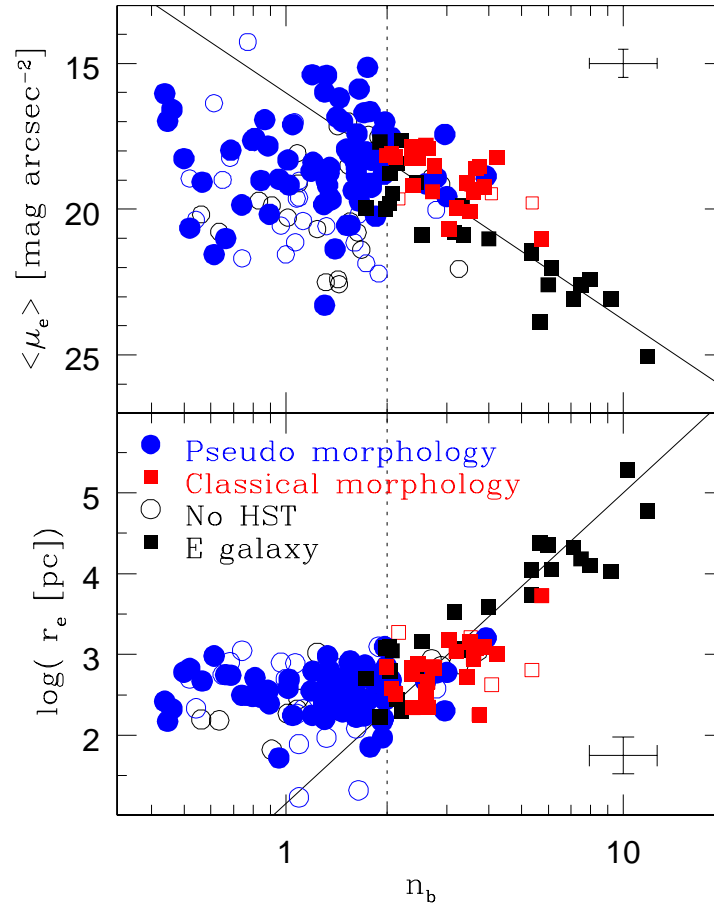


Fig. 1.4 The above figure, adapted from Fisher & Drory (2010), shows the correlation of bulge Sérsic index with structural properties of bulges. There is a clear and distinct break in these correlations at Sérsic index of $n_b = 2$. This break is consistent with a picture in which bulges with larger Sérsic index ($n_b > 2$) are physically similar to elliptical galaxies, and those with smaller Sérsic index ($n_b < 2$) are a different class of object.

and those galaxies that are poorly resolved, the correlation improves still. In this case only 4% of classical bulges have $n_b < 2$.

Exactly at what resolution the use of Sérsic index becomes unreliable is difficult to say. Nonetheless, even with the very loose cut applied here we already detect a difference in Sérsic index. As mentioned above, fitting Sérsic functions to galaxy light profiles is a very degenerate procedure. If a bulge diameter approaches the beam width of the data set, clearly using Sérsic index to diagnose bulge types would be unreliable in this scenario. Thus, if bulges are typically ~ 2 kpc in diameter, then surveys using SDSS only to measure bulge properties should not extend beyond

$z = 0.03$ or a distance of ~ 120 Mpc, in which a seeing of 1.5 arcseconds would allow for a few resolution elements to sample the bulge.

We remind the reader that this correlation is an empirical result. Broadly speaking, the observation that pseudobulges would have nearly-exponential surface brightness profiles, and thus be more similar to what is observed in disks, is consistent with the general observation that pseudobulges are disk-like. Yet, the physical reason that such a sharp dividing line in Sérsic index at $n_b = 2$ exists separating bulges of different morphological types, is not well understood. Furthermore, the exact distribution of Sérsic indices for pseudobulges and classical bulges is hard to establish for multiple reasons. First, if classical bulges and elliptical galaxies are truly a single class of object, then ellipticals should be included in any analysis of surface brightness profiles. Including early-type galaxies would lead to more galaxies with larger Sérsic index (Caon et al., 1994; Kormendy et al., 2009; Blanton et al., 2005). Secondly, galaxies in which both a pseudobulge and classical bulge are present would complicate this analysis. Such systems have been estimated to make up $\sim 10\%$ of bulge-disk galaxies (Fisher & Drory, 2010). Thirdly, it is difficult to compile large samples of unbiased pseudobulge identification methods that are independent of the Sérsic index. Nuclear morphology enabled by the HST archive and Sérsic index are the most widely available sources of pseudobulge detection. It is difficult to obtain, for example, kinematics with sufficient spatial and spectral resolution on a large number of galaxies. Also, as we will discuss later using star formation rates and/or stellar populations is subject to biases in the detected systems.

The correlations of structural properties with Sérsic index show a distinct change at $n_b = 2$ Fisher & Drory (2008, 2010). In Fig. 1.4 we show the correlation of bulge Sérsic index with half-light radius and effective surface brightness. Bulges with $n_b > 2$ show behavior consistent with that of E-type galaxies, that is to say a positive correlation between galaxy size (or luminosity) and Sérsic index (e.g. Graham et al., 1996; Khosroshahi et al., 2000; Kormendy et al., 2009; Falcón-Barroso et al., 2011). Bulges with $n_b < 2$ do not participate in these correlations, and in fact show a lack of scaling relationships between n_b and other structural quantities. This is clearly evident in $r_e - n_b$ parameter space.

In following sections we will discuss in more detail the correlations of bulge Sérsic index with kinematic, interstellar medium, and stellar population properties of bulges. Bulges with $n_b < 2$ are observed to have higher fractions (and surface density) of gas (Fisher et al., 2013), that is more actively forming stars (Fisher et al., 2009; Gadotti, 2009; Fisher & Drory, 2010), and has more disk-like kinematics (Fabricius et al., 2014) when compared to bulges with $n_b > 2$. These results, and those in Fig. 1.4, suggest that the Sérsic index is sensitive to physical differences between bulge types.

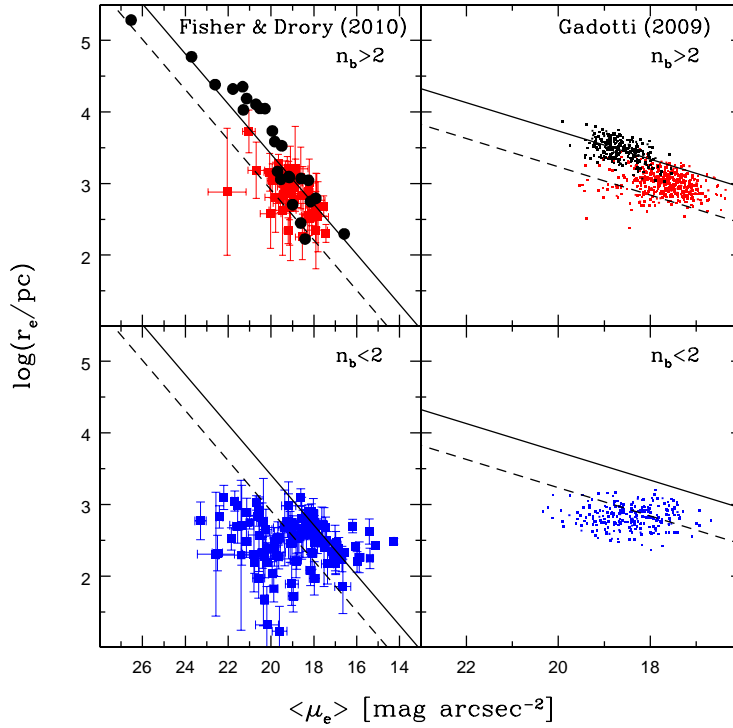


Fig. 1.5 Here we show the relationship of $\langle \mu_e \rangle - r_e$ for bulges (red & blue squares) and elliptical galaxies (black circles) using data from composite profiles of HST/NICMOS, Spitzer $3.6 \mu\text{m}$ and 2MASS data (the magnitude scale is set to match $3.6 \mu\text{m}$ scale) from Fisher & Drory (2010) (left), and SDSS i Gadotti (2009) (right). In both cases we show a correlation fit to the ellipticals (solid line) and a line set to contain the spread in elliptical galaxies (dashed line). The results of these studies are essentially consistent, there is a significant population of bulges that deviates toward lower surface brightness from this projection of the fundamental plane.

1.3.2 Differences in bulge types fundamental plane parameter space

Elliptical galaxies follow a very well-known set of correlations between surface brightness, radius, and velocity dispersion, known as the “fundamental plane” (Djorgovski & Davis, 1987; Faber et al., 1989; Kormendy, 1977a; Bender et al., 1992). These relationships are derived from the assumption that elliptical galaxies are virialized systems, with small - but significant - deviations corresponding to variation in mass-to-light ratios and the non-homology of such galaxies. Because simulations predict that structural scaling relations like the fundamental plane are likely to emerge through the merging processes that form elliptical galaxies through violent relaxation (e.g. Boylan-Kolchin et al., 2006), it would seem reasonable that

if pseudobulges, which are more disk-like, form significantly differently than elliptical galaxies and classical bulges they would not necessarily occupy the same correlation.

There is, however, a danger to using the fundamental plane to identify bulge types. There is no independent theory that predicts the location of pseudobulges in these correlations, and there is nothing to say that in certain projections of fundamental plane correlations pseudobulges and classical bulges would not overlap. We will continuously argue throughout this review, there does not seem to be a single ideal way to identify pseudobulges and classical bulges. A comprehensive approach that combines multiple indicators of bulge types is therefore called for.

Carollo (1999) shows that the centers of spiral galaxies that contain pseudobulges have lower surface density than classical bulges. The location of bulges in projections of the fundamental plane is studied with larger samples using full bulge-disk decomposition in Gadotti (2009) and also Fisher & Drory (2010). Both of these works find results that are consistent with Carollo (1999), that is a population of bulges with lower surface brightness than corresponding elliptical galaxies of similar size or luminosity.

In Fig. 1.5 we show the relationship between $\langle \mu_e \rangle$ and r_e (Kormendy, 1977a). The data set we use in this figure is taken from Fisher & Drory (2010) (left panels) and Gadotti (2009) (right panels). The data set from Fisher & Drory (2010) is considerably finer spatial resolution and uses near-IR data less affected by variations in mass-to-light ratios and extinction. The Gadotti (2009) sample is a much larger, uniformly selected sample of nearly 10^3 galaxies from SDSS, and therefore offers a statistically sound data set. Both of these studies find essentially the same result, a significant fraction of bulges deviates toward low surface brightness. Furthermore, those bulges that deviate from this relation are much more likely to have low Sérsic index. Based on these results, reproduced in Fig. 1.5, it is clear that if a bulge deviates significantly toward low surface brightness from the Kormendy (1977a) relation, then this is strong evidence that this bulge is a pseudobulge.

Identifying bulges as classical bulges because they are consistent with the $\langle \mu_e \rangle - r_e$ relationship, however, is less robust. Gadotti (2009) marks bulges contained within the spread of the Kormendy (1977a) relation as classical bulges. They argue that at least in this parameter space, these bulges are structurally similar to elliptical galaxies. This makes the assumption that other physical processes cannot make a bulge with similar values of surface brightness and size. Absent a result from simulations, we cannot know if that assumption is true.

We can look at the properties of those bulges that are consistent with the Kormendy (1977a) relation to determine how homogenous a class they are. In Fig. 1.6 we show the distribution of $3.6 - 8.0 \mu\text{m}$ color (Fisher & Drory, 2010) and $D_n(4000)$ (Gadotti, 2009) for the bulges that are consistent with the Kormendy (1977a) relation. Larger values of $3.6 - 8.0 \mu\text{m}$ color imply more active star formation per unit stellar mass. Smaller values of $D_n(4000)$ imply younger stellar populations; for display purposes we plot the $D_n(4000)$ values in reverse order, so in both panels younger, more star forming systems are on the right side of the panel. In both samples it is clear that selecting bulges only by the location in $\langle \mu_e \rangle - r_e$

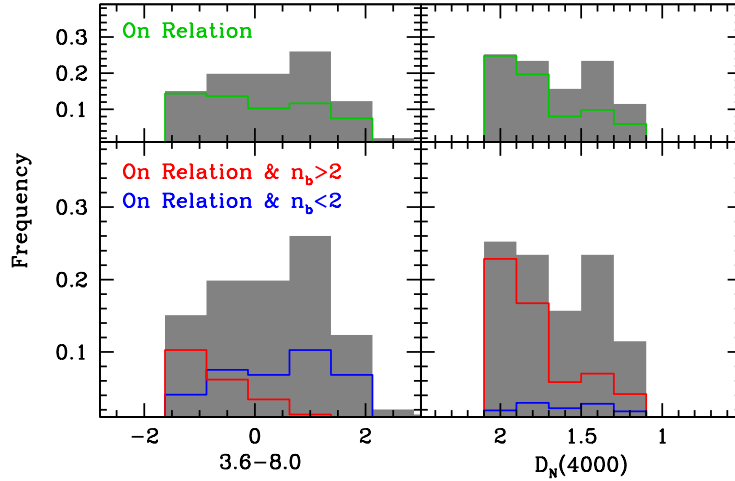


Fig. 1.6 The above figure aims to examine the properties of bulges that are consistent with the $\langle \mu_e \rangle - r_e$ relationship shown in Fig. 1.5. The left panels show distribution of 3.6 – 8.0 micron colors from Spitzer IRAC data, measured in Fisher & Drory (2010). Higher values of 3.6 – 8.0 indicate, roughly speaking, larger specific star formation rates. The left panels show $D_n(4000)$ values for bulges (excluding E galaxies) from Gadotti (2009). Smaller values of $D_n(4000)$ indicate younger populations. Note that we have inverted the x-axis of $D_n(4000)$ so that in all panels younger, higher star forming bulges are on the right side of the panel. The grey shaded region shows the distribution for the entire sample. The green line represents all those bulges that are consistent with the $\langle \mu_e \rangle - r_e$ relationship. The blue line is those bulges that are consistent with the $\langle \mu_e \rangle - r_e$ and have $n_b < 2$. The red line shows the distribution for bulges consistent with $\langle \mu_e \rangle - r_e$ and have $n_b > 2$.

parameter space does not uniquely separate bulges. In the bottom panel we show the combination of using both the Kormendy (1977a) relation and n_b as selection criteria for bulge types. In the Fisher & Drory (2010) sample this more cleanly identifies classical bulges as non-star forming systems.

In summary, using the fundamental plane as bulge type diagnostic carries certain caveats. If a bulge significantly deviates toward lower surface brightness from the Kormendy (1977a) relationship between $\langle \mu_e \rangle$ and r_e , then this is strong evidence that that bulge is a pseudobulge, based on studies of its star formation rate, Sérsic index, and nuclear morphology. However, if a bulge has parameters consistent with the fundamental plane, from an empirical point-of-view we cannot say what type of bulge this is. For example, if the aim of a study is to isolate a sample of bulge-disk galaxies that resemble M 31 (a prototypical classical bulge), then using $\langle \mu_e \rangle - r_e$ alone is clearly insufficient, and as we show in Fig. 1.6 this method selects a number of star forming bulges. Also, Fisher & Drory (2010) show that a number of bulges that are consistent with the Kormendy (1977a) relationship have nuclear morphology that, unlike M 31, resembles a disk.

1.4 The interstellar medium and stellar populations of pseudobulges and classical bulges

Historic work concluded that bulges are uniformly old and devoid of star formation (e.g. Whitford, 1978). This led to the widely held view that all bulges are old and inactive. This turns out to be true for some bulges, but it is not universally true by any means. For example, in the prototypical classical bulge of M 31, the dust SED is consistent with being completely heated by the old stars, and shows no evidence for new star formation (Draine et al., 2014), and also the stellar populations indicate a uniformly old population of stars, with mean ages above 12 Gyr (Saglia et al., 2010). However, work in the last 15-20 years shows that many bulges contain cold gas, actively form stars and can have short mass doubling times, and often have intermediate-to-young light-weighted stellar ages.

Peletier & Balcells (1996) show that some bulges are indeed quite blue, and that in general bulges have similar optical colors as the surrounding disk. Similarly, Regan et al. (2001) finds using interferometric observations of CO(1-0), that some bulges are as gas rich (from L_{CO} -to- L_{K} ratios) as the associated outer disk. In the past 10 years data from Spitzer Space Telescope, GALEX UV telescope, and CO interferometry from BIMA, OVRO, CARMA & PdBI have greatly improved our ability to measure star formation rates in bulges. We can now robustly say that specific star formation rates and gas fractions in the bulge region of nearby galaxies are often very high (Sheth et al., 2005; Jogee et al., 2005; Fisher, 2006; Fisher et al., 2009; Fisher & Drory, 2011; Fisher et al., 2013). Also, bulges can contain young stellar populations (Gadotti & dos Anjos, 2001; MacArthur et al., 2004; Peletier et al., 2007; Ganda et al., 2007). See also Kormendy & Kennicutt (2004) for a review.

From a physical perspective it makes sense that pseudobulges would be systematically younger with more active star formation than classical bulges. The present model is that classical bulges formed in the early Universe, either through merging (Aguerre et al., 2001; Robertson et al., 2006) or as the result of clumpy disk instabilities (Noguchi, 1999; Elmegreen et al., 2008). The former become less frequent, and the latter are extremely rare below $z \sim 1$. Conversely, galaxies with pseudobulges either did not experience these processes, or they were significantly less pronounced, the resulting galaxy was able to evolve secularly for long periods of time and still does. Some of them still contain significant amount of gas to fuel internal evolution of the bulge. Also, the presence of a classical bulge may in fact stabilize a galaxy against star formation, and especially the secular inflow of gas (Martig et al., 2009). This process known as “morphological quenching” may act to reinforce a correlation with bulge structural properties and bulge star formation rates.

Before going on, we must point out a simple, yet critical, caveat to using stellar populations, star formation rates, and gas fractions to identifying pseudobulges. Gas stripping by cluster environments (as described by Kenney et al., 2004) can shut down star formation in a galaxy. If such a galaxy had previously formed a pseudobulge, that bulge would quickly appear inactive and old. Also, simulations show that pseudobulges can form in dissipationless systems (Debattista et al., 2004). It is

therefore important that one should not use the absence of star formation alone as a reason to suggest a galaxy does not contain a pseudobulge.

To be clear, when we refer to “bulge” star formation rates and gas masses what we really mean is the star formation rate (or gas mass) inside the region of the galaxy where the bulge dominates the light. Cold gas, and thus star formation, happens in a thin disk (García-Burillo et al., 1999) of scale height of ≤ 100 parsecs. Bulge-disk decompositions, however, do not typically consider the thickness of the bulge. Indeed, the thickness of pseudobulges is very poorly constrained. Some are likely very thin (as argued by Kormendy, 1993), however, given the common presence of resonant phenomena it is likely that many are thickened. If the goal is to understand how properties of the bulge evolve, however, then comparing the entire mass (or luminosity) of the bulge stars to the entire rate of star formation in a bulge seems appropriate.

1.4.1 A brief aside on measuring star formation rates in bulges

The measurement of star formation rates in galaxies, SFR , is typically done by means of a tracer of the amount of young stars present. This field has greatly advanced in the past decade Kennicutt (1998); Calzetti et al. (2007); Kennicutt et al. (2009); Leroy et al. (2012); Kennicutt & Evans (2012). Because the emission from O and B stars heavily dominates the UV spectral range, it is straightforward to argue that $SFR \propto L_{UV}$. The calibration of such a relationship can be found in Salim et al. (2007). For bulges, data from the GALEX UV space telescope is well suited to resolve ~ 1 kpc in galaxies within 40 Mpc. An alternative approach is to use emission from HII regions, typically this is done using the $H\alpha$ flux, assuming in this case that $SFR \propto L_{H\alpha}$.

A difficulty to estimating the emission from young stars is that dust absorbs UV/optical emission. This is especially important for galaxy centers (i.e. bulge regions), which experience more extinction (Peletier et al., 1999; MacArthur et al., 2004). In fact, we know from studies of our own galaxy that star formation can occur in heavily obscured regions (for review Evans, 1999; Kennicutt & Evans, 2012), and therefore much of the light may be missed in optical observing campaigns.

One way to overcome the effects of extinction would be to measure the flux of a Hydrogen emission line in the near-infrared range (e.g. Pa α emission). However, such measurements can be difficult to make, and are often low signal-to-noise. Alternatively, data from *Spitzer Space Telescope* allows us to directly probe the re-radiation in the infrared of the energy absorbed by the dust in the UV/optical, for example using emission at $24 \mu\text{m}$ (Calzetti et al., 2007). A common approach in the current literature is to combine different star formation tracers (e.g. Kennicutt et al., 2009) to account for both the unobscured star formation (traced by UV or $H\alpha$) and the obscured star formation (traced by infrared emission).

The $8 \mu\text{m}$ emission is dominated by polycyclic aromatic hydrocarbons (often called PAHs). At present, and with respect to measuring the properties of bulges, a

significant advantage of $8\ \mu\text{m}$ maps available from Spitzer is that they have significantly finer spatial resolution (beam size of Spitzer IRAC $8\ \mu\text{m}$ data is ~ 2 arcsec, roughly 3 times better than $24\ \mu\text{m}$ maps with MIPS). However, flux from the $8\ \mu\text{m}$ emission is not reliable as a direct, one-to-one, indicator of the star formation rate. Calzetti et al. (2007) show that the correlation between continuum-corrected $8\ \mu\text{m}$ flux and Pa α flux depends on both environment and metallicity. In light of this, we limit our use of PAH emission to mostly an on/off metric of activity, separating star forming bulges (bright $8\ \mu$ emitting bulges) from non-star forming systems.

A second issue in measuring star formation in galaxy bulges is the contamination of the metrics of star formation by old stars. Old stellar populations make a measurable contribution of light at UV wavelengths and lead to an overestimate of the star formation rate (e.g. Cortese et al., 2008). Also, old stars can heat dust and thereby increase the $24\ \mu\text{m}$ flux. These problems are especially pronounced in bulges where the surface density is very high. In this case the flux in tracers used to probe star formation is actually a combination of contributions from old and young stars. Leroy et al. (2012) study this in galaxy disks by modelling the diffuse emission. They find that typically roughly 20% of the emission at $24\ \mu\text{m}$ can be attributed to evolved stellar populations. Fisher et al. (2013) investigate bulges specifically and find similarly that in typical star forming bulges the star formation rate is decreased by roughly 20% when accounting for old stellar populations. Both Leroy et al. (2012) and Fisher et al. (2013) show that this effect is stronger in regions of low star formation. Fisher et al. (2013) also shows, as expected, that this effect is more pronounced when the surface density of star light is higher. For example, in the bulge of M 31, Draine et al. (2014) find that essentially all of the dust emission is accounted for by heating by stellar populations.

1.4.2 Active star formation and more gas is strongly correlated with bulge types

Though there is a long history of evidence that many bulges are actively forming stars, and that star formation is likely significantly altering the stellar structure of a bulge (Kormendy & Kennicutt, 2004, for review, and outlined above)[], direct comparisons to bulge classifications began mostly recently. A general summary is that if a bulge is star forming, statistically speaking it likely has other pseudobulge properties (e.g. $n_b < 2$, disky nuclear morphology). Conversely, if a bulge is not star forming it can have a large mix of properties, consistent with the discussion above. Also, a small subset of galaxies have star forming centers, but quiescent disks; these systems also have large bulge Sérsic index. A plausible scenario to explain these systems could be the recent accretion of a satellite directly into the galaxy center (e.g. Aguerri et al., 2001).

Fisher (2006) uses data from Spitzer Space Telescope and archival HST data to directly compare the morphological diagnosis of bulge types to the $3.6 - 8.0\ \mu\text{m}$ color profiles of galaxies with pseudobulges and those with classical bulges. In this

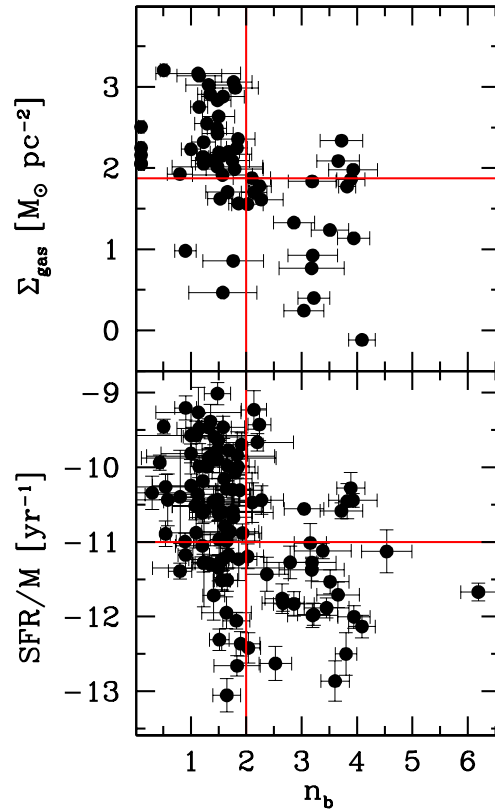


Fig. 1.7 The above figure compares the specific star formation rate (bottom panel) and gas surface density (top panel) of bulges to the bulge Sérsic index. Data are taken from Fisher et al. (2009); Fisher & Drory (2011); Fisher et al. (2013). The vertical lines indicate the commonly used pseudo-classical bulge dividing line of $n_b = 2$, the vertical lines are set to guide the eye for $SFR/M = 10^{-11}$ yr and $\Sigma_{\text{gas}} = 75 M_{\odot} \text{pc}^{-2}$.

case, $3.6 - 8.0 \mu\text{m}$ color is a very rough proxy for specific star formation rate (star formation rate divided per unit stellar mass). They find that in galaxies with classical bulges, the color of the disk indicates active star formation, however there is a sharp break near ~ 1 kpc where the color profile transitions to a non-starforming bulge. In contrast, there is no such transition in galaxies with pseudobulges. The pseudobulge is forming stars similarly to the outer disk. Fisher & Drory (2010) follow this up by calculating the $3.6 - 8.0 \mu\text{m}$ color for ~ 180 galaxies, and study other indicators of bulge type (morphology, Sérsic index, and $\mu_e - r_e$). They find that if a bulge has mid-IR colors satisfying $3.6 - 8.0 > 0$, then that bulge has properties that resemble a pseudobulge (eg. low n_b).

In Fig. 1.7, we compare the specific star formation rate and gas surface density of bulges to the bulge Sérsic index, using data from Fisher et al. (2009), Fisher & Drory (2011), and Fisher et al. (2013). The results here re-iterate the results of these papers. In both panels, it is clear that active star formation and high surface densities of gas are exclusively found in bulges with low Sérsic index. It is worth pointing out that there is no *a priori* reason that the bulge Sérsic index would correlate with the bulge gas density; a similar correlation is recovered if one measures bulge gas density with a fixed radius (e.g. 500 pc) and if one uses the bulge radius as done here. These correlations imply that the separation of bulge types is likely tied to a physical distinction. The results in Fig. 1.7 continue to motivate that the separation of bulges into at least two categories is informative to the physics of galaxy evolution.

Using the star formation rate (or gas surface density) of a bulge alone to identify it as a pseudobulge or classical bulge is, statistically speaking, somewhat ambiguous. 8% of bulges that have active star formation (defined as $SFR/M > 10^{-11} \text{ Gyr}^{-1}$) also have n_b that is significantly larger (considering error bars) than $n_b = 2$. A similar result is true when considering $\Sigma_{\text{gas}} > 75 M_{\odot} \text{ pc}^{-2}$. Therefore, if one discovers that a bulge has a very active gas rich center, this is strong evidence for that bulge being a pseudobulge. However, it is clear that when the star formation or gas density is low, one should not infer the bulge type. We recommend using star formation as a “second tier” method for identifying pseudobulges and classical bulges. For example if other metrics give ambiguous results but the bulge is very actively forming stars one could then conclude the bulge is a pseudobulge.

1.4.3 Stellar population indicators and bulge types

Stellar population indicators in bulges show a wide range in properties (for a brief review see Peletier, 2008). The topic of stellar populations is quite broad with a large variety of techniques and results that could easily fill its own review. We will concentrate on those results in which correlations, or the notable lack thereof, are relevant as diagnostics of bulge type. There is no set of stellar population parameters that is typical of a bulge. As mentioned before, an overwhelming majority of studies shows that the historic assumption that all bulges are uniformly old is simply not supported by the data (e.g. de Jong, 1996; Peletier & Balcells, 1996; Carollo et al., 2001; Proctor & Sansom, 2002; Moorthy & Holtzman, 2005).

There has been mixed evidence that optical color can be used as a means of identifying pseudobulges. Early results were promising. For example, Peletier & Balcells (1996) found a large spread in ages of bulges, and that average stellar age of bulges correlates with that of disks (young bulges are in young disks). This was confirmed in a much larger samples by Gadotti & dos Anjos (2001); MacArthur et al. (2004). Carollo et al. (2001) find that the average $V - H$ color of exponential bulges with diskly nuclear morphology (i.e. pseudobulges) is bluer than that of $r^{1/4}$ bulges.

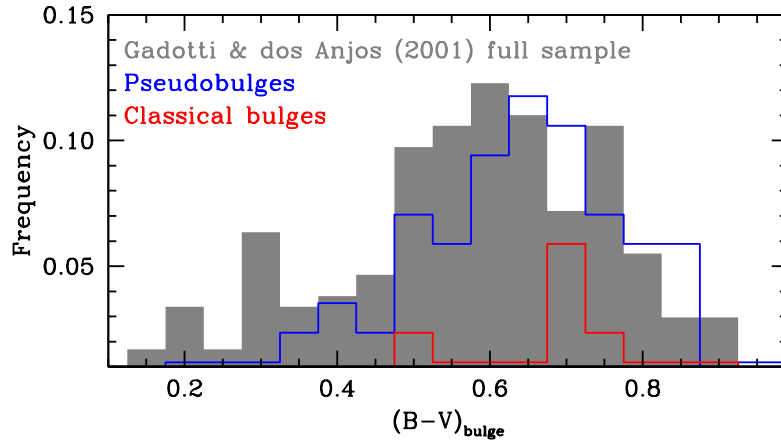


Fig. 1.8 Distribution of $B - V$ for bulges in the Gadotti & dos Anjos (2001) sample of galaxies (shaded region). The blue line represents those bulges that are identified as pseudobulges and the red line represents those that are classified as classical bulges (by combining Sérsic index, nuclear morphology and the Kormendy relationship). Though classical bulges are rarely found to be blue, pseudobulges very often have red optical colors.

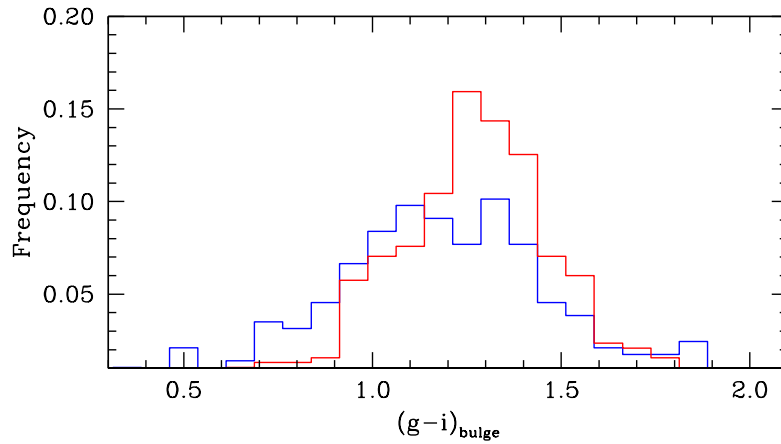


Fig. 1.9 Distribution of $g - i$ for bulges in the Gadotti (2009) sample of galaxies. The blue line represents those bulges that are identified as pseudobulges and the red line represents those that are classified as classical bulges (by combining Sérsic index, and the Kormendy relationship).

Studies of the color of larger samples of bulges suggest that a single broadband color using optical or near infrared filters do not correlate strongly enough with other indicators of pseudobulges for reliable use. In Fig. 1.8 we show the distribution of bulge colors from Gadotti & dos Anjos (2001) (grey shaded area). We also cross-reference the sample from Fig. 1.3 against 3 papers which contain samples of the same bulge color (Gadotti & dos Anjos, 2001; Möllenhoff, 2004; Fisher et al., 2013)¹. Pseudobulges are identified as bulges which have any of the following: $n_b < 2$, nuclear morphology that resembles a disk, and/or low surface brightness outliers from $\mu_e - r_e$ relation. The Gadotti & dos Anjos (2001) sample is shown to ensure that our bulge classification sample is not significantly biased. The distribution of classical bulges clearly skews to the redder colors, similar to Carollo et al. (2001). Blue bulges are far more likely to be pseudobulges. However unlike the previous methods of identifying pseudobulges there is not a significant range in this parameter over which classical bulges are not found.

The lack of a strong correlation between bulge color and type is likely not due to sample selection. Gadotti (2009) finds a similar result using $g - i$ colors. In Fig. 1.9 we show the distribution of bulge colors for the 670 bulge-disk galaxies from Gadotti (2009). Fernández Lorenzo et al. (2014) find a similar result with 189 galaxies, albeit the sample is biased only to include isolated galaxies.

Gadotti (2009) also compare the stellar populations tracer $D_n(4000)$ (Kauffmann et al., 2003) to bulge types (determined from bulge-disk decompositions). The break in the optical spectrum which occurs at 4000 Å is smaller for younger stellar populations (Bruzual A., 1983; Kauffmann et al., 2003, for description see), and is a good identifier of young or bursty populations. Gadotti (2009) find indeed that pseudobulges have on average smaller values of $D_n(4000)$ and therefore pseudobulges are more likely to be young, but again there is not a significant range that isolates one type of bulge.

Taken all together, these results suggest that there tends to be a preference for pseudobulges to be blue *on average* compared to classical bulges. This particular subject could benefit from a work with both a well-defined and large sample of galaxies that is well resolved. However, based on the data that presently exists, optical color on its own is not a reliable indicator of bulge-type.

Similar to the results from optical colors, studies of bulge ages using more robust techniques such as absorption line indices or spectroscopic synthesis, return mixed results (see Renzini, 2006 and references therein for a discussion of these techniques). Proctor & Sansom (2002) shows that bulges are younger on average and have fewer metals than early type galaxies. Both Moorthy & Holtzman (2005) and Thomas & Davies (2006) find a wide spread in ages, and that many bulges in later type (Sb-Sbc) galaxies are quite old. MacArthur et al. (2009) find, similarly, that the fraction of mass in bulges that was formed in the past gigayear is quite small. Zhao (2012) uses the Sloan Digital Sky Survey to measure the stellar populations of bulges in a sample of 75 isolated galaxies. Bulge types are diagnosed using both Sérsic index and the $\mu_e - r_e$ relation, and they find that on average pseudobulges

¹ Fisher et al. (2013) use SDSS $g - r$, which we convert to $B - V$ via Smith et al. (2002) transformations.

have more prolonged star formation than classicals. Zhao (2012) find no classical bulges that are younger than ~ 6 Gyr (mass weighted age), conversely roughly 30% of pseudobulges are found to be younger than this. However, the average age difference between the two populations of bulges is not very large.

Differences in stellar population indicators do exist between the bulges of different types. A particularly significant difference is found in the absorption line indices of bulges (Peletier et al., 2007; Ganda et al., 2007). It is well known that for elliptical galaxies the $Mg\ b$ line index correlates well with velocity dispersion (e.g. Bender et al., 1992). Peletier et al. (2007) and Ganda et al. (2007) show that many bulges fall below this relation, especially those bulges with low velocity dispersion centers and/or those bulges in late-type galaxies.

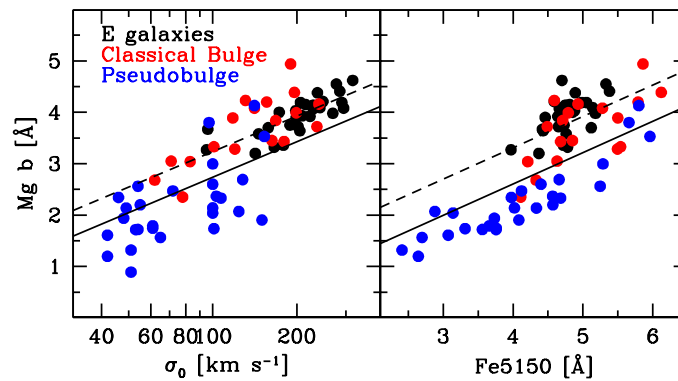


Fig. 1.10 The $Mg\ b - \sigma$ relationship for elliptical galaxies and bulges. We have restricted the control sample (black dots) to only the E galaxies from the SAURON sample to ensure that no pseudobulge galaxies are included. We take the bulge values from Peletier et al. (2007) and Ganda et al. (2007). Quantities for pseudobulges (identified with nuclear morphology, Sérsic index and the $\mu_e - r_e$ relation) are plotted as blue points, and the red points represent classical bulges. The dashed line is offset $0.5\ \text{\AA}$ below the best fit relation (solid) line. Only pseudobulges are found below this line.

In Fig. 1.10 we show that a strong connection exists between bulge type and absorption line indices, specifically $Mg\ b$ and Fe5150. For this figure we show the central values of pseudobulges, classical bulges and elliptical galaxies taken from a sample combining data from Ganda et al. (2007); Peletier et al. (2007); Kuntschner et al. (2010). We have classified bulges using bulge Sérsic index and bulge morphology. No classical bulge or elliptical galaxy has $Mg\ b < 2.35\ \text{\AA}$, conversely over $2/3$ of pseudobulges have lower values. (See Ganda et al., 2007; Peletier et al., 2007; Kuntschner et al., 2010 for a discussion of these Lick indices.) Similarly, the lowest value of Fe5150 in classical bulges and elliptical galaxies is $3.97\ \text{\AA}$ whereas roughly 50% of pseudobulges are found below this limit. As we show in Fig. 1.10, the Lick indices become particularly powerful when combined with the velocity dispersion. In each panel the dashed line is a best fit relationship to

the E galaxies and classical bulges, the solid line represents a relation with the same slope, yet offset down in Mg b such that it separates pseudobulges and classical bulges.

Based on this data set a bulge is a pseudobulge if it meets any of the following criteria:

1. $\text{Fe}5150 < 3.95 \text{ \AA}$,
2. $\text{Mg b} < 2.35 \text{ \AA}$,
3. $\Delta \text{Mg b} < 0.7 \text{ \AA}$ compared to the $\text{Mg} - \sigma$ correlation,
4. $\Delta \text{Mg b} < 0.7 \text{ \AA}$ compared to the $\text{Mg} - \text{Fe}$ relation.

All low Mg b outliers to the $\text{Mg} - \sigma$ relation are also outliers to the $\text{Mg} - \text{Fe}$ relation, but the reverse is not true. Conversely, there is more spread in the classical bulges in $\text{Mg} - \text{Fe}$. We also stress that because the sample of bulges includes a number of old S0 galaxies from the SAURON survey, using these Lick indices to identify pseudobulges and classical bulges appears to be robust against age. So it seems that using both of these relationships together would be a powerful tool for identifying pseudobulges, especially in the near future in which surveys such as SAMI and MANGA will measure absorption line strengths for large numbers of galaxies.

1.5 Identifying Pseudobulges and Classical Bulges with Kinematic Properties

Kinematic measurements of bulges provided some of the earliest evidence for the dichotomous nature of bulges. Kormendy (1982) points out that some bulges in barred disks are kinematically more similar to disks than those in unbarred disks. This kinematic similarity is indicated by the ratio of peak rotation velocity to bulge velocity dispersion, which is taken as a proxy of the ratio of “ordered-to-random motions.” Indeed, use of the $V/\sigma - \epsilon$ parameter space can distinguish pseudobulges from classical bulges, as shown by (Kormendy, 1993; Kormendy & Kennicutt, 2004; Kormendy & Fisher, 2008). However, these studies rely on very small samples, fewer than 20 bulge-disk galaxies, and are thus difficult to control. At present, it is safe to say that bulges with values well above the “oblate line” in the $V/\sigma - \epsilon$ parameter space are considered to be rotating bulges, and thus from a theoretical perspective would be “pseudobulges”, but it is difficult to estimate empirically, using currently available data, how often a bulge that has low Sérsic index would also be found in the “disk” region of the $V/\sigma - \epsilon$ diagram.

Central velocity dispersion alone does not completely separate bulge types. The distribution of σ_0 for a sample of ~ 100 S0-Sc galaxies is shown in Fig. 1.11. To construct the kinematic sample we use data from published sources that have sufficient velocity resolution to measure the central dispersion of bulges ($\sigma_{\text{bulge}} \geq 50 \text{ km s}^{-1}$), and also have sufficient spatial resolution to isolate the absorption line kinematics in the bulge region ($r_{\text{bulge}} \sim 1 \text{ kpc}$) that also have available bulge-disk decompositions from the sample used in Fig. 1.3 of this review. We use velocity

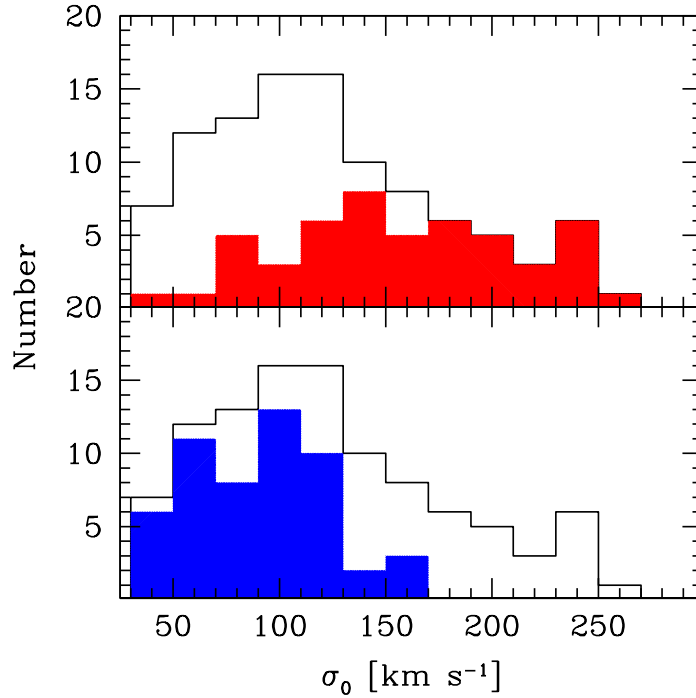


Fig. 1.11 Distribution of central velocity dispersions for galaxies with published σ_0 in the sample from Fig. 1.3. As before, pseudobulges are indicated by blue shaded region, and classical bulges by red. There is clearly significant overlap between the two samples.

dispersions from Héraudeau et al. (1999); Barth et al. (2002); Ganda et al. (2007); Kuntschner et al. (2010); Fabricius et al. (2012). In this comparison we identify pseudobulges as having $n_b < 2$ or prominent disk-like nuclear morphology as described earlier. Zhao (2012) finds that the distribution of central velocity dispersions of pseudobulges is essentially the same when they identify pseudobulges using Sérsic index or with the Kormendy relation. On average, pseudobulges have lower central velocity dispersion than classical bulges ($\langle \sigma_0 \rangle_{pseudo} \sim 90 \text{ km s}^{-1}$, compared to $\sim 160 \text{ km s}^{-1}$ for classical bulges). There is a strong decline in the number of pseudobulges with $\sigma > 130 \text{ km s}^{-1}$. However, roughly $\sim 1/3$ of the classical bulges in this sample have $\sigma < 130 \text{ km s}^{-1}$. It is for this reason σ_0 alone cannot be used to statistically isolate all pseudobulges from classical bulges. When a bulge has particularly high velocity dispersion ($\sigma > 130 \text{ km s}^{-1}$) then it is most likely a classical bulge.

A large sample of uniform measurements of velocity dispersion preferably with integral field spectroscopic measurements in bulge-disk galaxies would have significant value in understanding pseudobulge and classical bulge properties, nonetheless

the result in Fig. 1.11 does not appear to depend on the sample. Both Fabricius et al. (2012) and Zhao (2012) find essentially the same result that we report here.

Kormendy & Kennicutt (2004) shows that bulges that are low- σ outliers to the Faber & Jackson (1976) relation between bulge magnitude and velocity dispersion, are likely pseudobulges. However, there is a significant amount of spread in this correlation, and similar to the $\mu_e - r_e$ if a bulge is co-located in parameter space with this relationship it does not mean the bulge is a classical bulge.

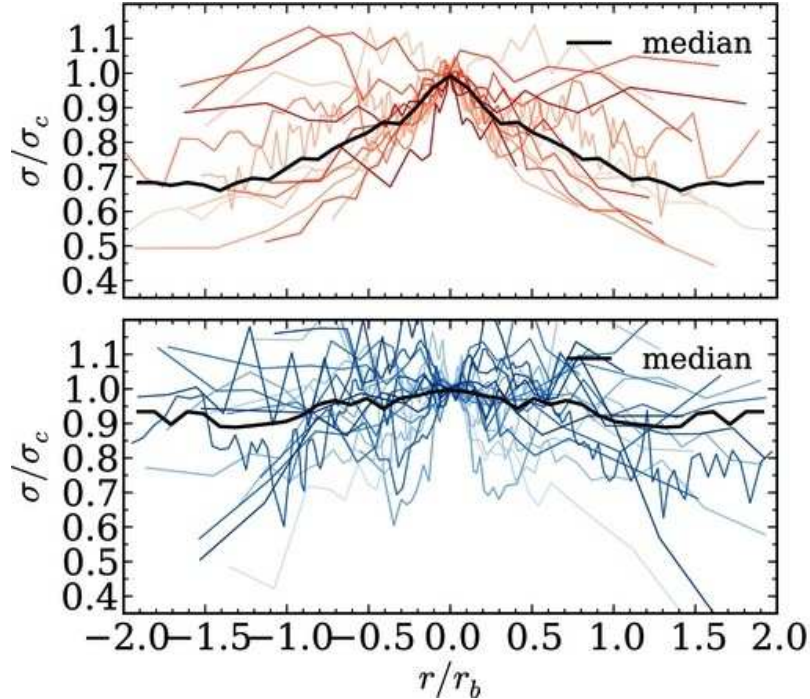


Fig. 1.12 Here we re-plot a result from Fabricius et al. (2012) that shows how the radial profile of the velocity dispersion in pseudobulges is much flatter than that found in galaxies with classical bulges.

Significant correlations between bulge type and the radial structure of kinematics have been seen by a number of authors (e.g. Falcón-Barroso et al., 2006; Comerón et al., 2008; Fabricius et al., 2012). In Fig. 1.12 we show the basic result (in this case taken from Fabricius et al., 2012) that galaxies with classical bulges have centrally peaking velocity dispersion profiles, where galaxies with pseudobulges do not. For this result, Fabricius et al. (2012) identifies pseudobulges using Sérsic index and bulge morphology. This is consistent with the overall picture of classical bulges and pseudobulges. In this case a classical bulge is considered to be a separate component from the disk, and the classical bulge is dynamically hotter

than the disk. In the center of the galaxy the classical bulge dominates the light and the measured kinematics. At large radius the disk dominates the light, and measured kinematics have lower dispersion. The intermediate radii show the transition between these two regimes. Pseudobulges, conversely do not have a hotter separate component, they are often thought of simply as high surface density centers of disks, therefore kinematically they do not break from the behavior of the disk. Fabricius et al. (2012) quantifies the kinematic profile shape with the logarithmic derivative $d \log(\sigma)/d \log(r)$. The logarithmic derivative correlates well with bulge type. Galaxies with classical bulges ($n_b > 2$ and E-type morphology) have more negative values (i.e. more centrally peaking $\sigma(r)$).

Peletier (2008) notes that all the bulges with central velocity dispersion minima in the samples of Ganda et al. (2007) and Peletier et al. (2007) also are low-Mg b outliers (as described above). Comerón et al. (2008) studies the properties of so-called σ -drop galaxies (galaxies with a central minimum in velocity dispersion). They find that dusty structures that would, in this review, be classified as indicative of pseudobulges are very common in these galaxies. They also find a higher fraction of circumnuclear star formation in σ -drop galaxies.

Fabricius et al. (2012) shows that combining V/σ with metrics of the profile shape can be very powerful for identifying pseudobulges. Galaxies with classical bulges have low values of V/σ and central cuspy surface brightness profiles. Essentially the result is physically sound; if a bulge is dominated by dispersion and has a higher dispersion to the surrounding disk then it is almost always a classical bulge. Conversely, pseudobulges are not found in the same region of parameter space. Fabricius et al. (2012) finds that outliers to this rule tend to be galaxies that in line-of-sight velocity distributions that these galaxies have multiple kinematic components that are affecting the measurement of the shape of the velocity profile. The drawback to this method is that it requires sufficient velocity resolution to measure the kinematics of the disk, and therefore may be inaccessible to surveys such as MANGA and SAMI.

1.6 Composite Pseudo-Classical Bulges

Assuming that galaxies either have only a pseudobulge or a classical bulge is most likely an oversimplification. Bulges that consist of both a thin, starforming pseudobulge and a hot-passive classical bulge are very likely present in some galaxies. There has been very little work done on composite bulges. This is definitely an area that could use more work, though results, by the nature of the problem, are likely to be difficult to interpret.

Fisher & Drory (2010) argue that scaling relations can be used to identify some mixed-case bulges. Bulges that are high mass or high surface brightness outliers from fundamental plane scaling relationships are likely to be composite. In these systems, a classical bulge is assumed to be on a scaling relation, for example the $\mu_e - r_e$ correlation of E galaxies. The pseudobulge component increases the mass,

without strongly affecting the value for the effective radius. They use models to show that in the limit that the mass of the classical component is larger than that of the pseudo-component this is true. Fisher & Drory (2010) find that bulges that are co-located in fundamental plane parameter space with models of composite pseudo-classical bulges have lower specific SFR than the median pseudobulge, and also have $n_b \sim 1.8 - 2.1$. They show by modeling that adding a high Sérsic index bulge to a low Sérsic index pseudobulge tends to produce an intermediate range n_b . Fisher & Drory (2011) use these results to estimate that roughly 10-20% of bulges in the local 11 Mpc, fit this description. This is only a rough estimate. Much more work is needed to truly get a robust estimate of the frequency of composite bulge systems.

Erwin et al. (2015) uses stellar kinematics to model the internal structures of several examples of galaxies which contain both a pseudobulge and classical bulge. These models generally find a small compact structure which is referred to as a classical bulge, with a diffuse structure around it that has dynamics that are more consistent with disks, which they call the pseudobulge.

The take away is that the presence of a pseudobulge in a galaxy does not necessarily imply that there is not an old, dynamically hot component of stars within that system. In the future, as integral field spectroscopy becomes more common, dynamical modelling which places estimates on the maximum fractional mass of a hot stellar component in pseudobulges of ranging properties (B/T , SFR/M_{star} , n_b , etc.) may prove very useful.

1.7 Summary

In this review we have highlighted a number of observed properties that mark empirical differences between classical bulges and pseudobulges. We certainly do not always understand the underlying physical reason for these observed differences. For example, why $n_b \sim 2$ seems to be such a good dividing line between bulge types is not clearly understood. An alternate approach is to base diagnostic methods on physically motivated arguments (such as an assumption on the star formation history, or the structural properties). However, physically motivated arguments can be specious, especially when we consider that theoretical understanding of bulge formation is incomplete at best. For example, a decade prior to writing this review the most popular theory to explain the population of bulges was major mergers. At present, this is no longer an ubiquitously accepted theory, rather it is thought by many that some mixture of turbulent clump instabilities early on and secular evolution in more recent epochs combine to generate many bulge properties (e.g. Elmegreen et al., 2008; Genzel et al., 2008; Obreja et al., 2013).

Below, we summarize the empirically-determined properties of pseudobulges and subsequently classical bulges. A very important feature is that pseudobulge properties are not always the complement of classical bulge properties. For example, if a bulge is star forming (and there is no interaction present) this is very good evidence

that the bulge is a pseudobulge, but when the bulge is not star forming this does not imply the bulge is classical. It could be either pseudobulge or classical bulge.

The diagnostics are divided into two categories. Those in the top categories (or category I diagnostics) are properties in which the parameter shows a relatively clean separation between almost all pseudobulges and classical bulges. The category II diagnostics are those in which a range in parameter is only occupied by a single bulge type, however does not identify the whole population of bulges. If one wishes to statistically identify all bulges of a certain type in a sample, then a category I diagnostic should be used. Alternatively, if one has a single galaxy, or a sample of bulges and simply wishes to know if these are bulges of a certain type then category II diagnostics may be sufficient. For classical bulges there is a third category which are necessary, but not sufficient properties of classical bulges.

1.7.1 Observational Definition of Pseudobulges

Here we list the empirically-determined properties associated with bulges that resemble disks, i.e. pseudobulges.

I - Optical morphology in the region where the bulge light is dominant shows spiral or ring structure, when measured at high spatial resolution ($\text{FWHM} \leq 100$ pc). A description of this can be found in SS2.

I - Sérsic index of bulge stellar light profile in a bulge-disk decomposition is less than 2. Both Fisher & Drory (2008, 2010), also Fig. 1.3 of this review, show that the turnover in the distribution between classical bulges and pseudobulges is at $n_b \sim 2.1$, and below $n_b = 2$ almost no classical bulges are observed.

I - Correlations with absorption line strengths are very well connected to bulge types (Peletier et al., 2007; Ganda et al., 2007). As we show in Fig. 1.10, a bulge is a pseudobulge if $\Delta \text{Mg b} < 0.7 \text{ \AA}$ compared to either the correlations of Mg- σ or Mg-Fe. Below we discuss how the absolute value of absorption correlates with bulge type.

I- Velocity dispersion profile shape thus far is the best kinematic method to identify pseudobulges and classical bulges (Fabricius et al., 2012). A bulge is identified as a pseudobulge if the logarithmic derivative of the velocity dispersion profile is greater than $d \log(\sigma) / d \log(r) \geq -0.1$ and $\langle v^2 \rangle / \langle \sigma^2 \rangle \geq 0.35$. An extreme version of this result are the so-called σ -drop galaxies which have a local minimum in velocity dispersion that is located where the bulge is, these galaxies would have a positive value for $d \log(\sigma) / d \log(r)$, and thus be pseudobulges.

II - Low surface brightness outliers from scaling relations are found to be pseudobulges (Carollo et al., 2001; Gadotti, 2009; Fisher & Drory, 2010). However, many bulges that are co-located with fundamental plane projections also show evidence of being pseudobulges (low n_b , high SFR/M_{star} , Fisher & Drory, 2010 and Fig. 1.6. If a bulge is co-located with a projection of the fundamental plane, then

this does not discriminate between being a pseudobulge or a classical bulge.

II - **Specific star formation rate** can be indicative of bulge types. If the region in which the bulge dominates the light has $SFR/M_{star} \geq 10^{-11} \text{ yr}^{-1}$ then the bulge is very likely to be a pseudobulge (Fisher, 2006; Fisher et al., 2009). However, if the bulge is less active, where $SFR/M < 10^{-11} \text{ yr}^{-1}$, the bulge could be either a pseudobulge or classical bulge. Care should be taken also to determine if the galaxy is presently experiencing an interaction, in such cases correlations between SFR/M_{star} and other parameters, such as n_b become less robust.

II - **Absorption line strength** a bulge is found to be a pseudobulge if $\text{Fe}5150 < 3.95 \text{ \AA}$ and/or $\text{Mg b} < 2.35 \text{ \AA}$. In the sample of SAURON based observations presented in Fig. 1.10 (Peletier et al., 2007; Ganda et al., 2007), no classical bulge is found with absorption lines below this range. However, this selection does not include all pseudobulges, and therefore in a statistical study should be used in combination with other diagnostics.

II - **Low - σ outliers** to the Faber & Jackson (1976) relation between bulge magnitude and central velocity dispersion of the bulge are found by Kormendy & Kennicutt (2004) to be pseudobulges. However, if a bulge is co-located with the Faber & Jackson (1976), we cannot determine - from this information alone - if it is a pseudobulge or classical bulge.

II - **Extremely blue optical colors** statistically speaking optical color does not appear to be a good indicator of bulge type, however the small subset of bulges with very blue optical colors $B - V < 0.5$ are found to be pseudobulges, and classical bulges are rare for $B - V < 0.65$.

1.7.2 Observational Definition of Classical Bulges

We note again that classical bulges are not always the complement of pseudobulges. In some parameter spaces there is significant overlap between the two populations. This could be evidence of a bridging population, but it is also very likely that not every metric of galaxy properties is uniquely manifested by a single galaxy evolution mechanism.

The obvious condition is that first a classical bulge must not satisfy any of the criteria listed under the definition of pseudobulges.

I- **Optical Morphology** is found to be simple and free of spiral arms and nuclear rings in the region of the galaxy where the bulge dominates the light. It is important to have good resolution, preferably in the middle of the optical wavelength range ($\sim V$ through I bands). In all but the closest galaxies HST is necessary to diagnose bulge with their morphology.

I- **Sérsic Index** of classical bulges is found to be almost always greater than two, $n_b(\text{classical}) > 2$ (Fisher & Drory, 2008).

I - **Correlations between absorption line strengths** that are consistent with E galaxies is a property exclusively of classical bulges. Pseudobulges establish correlations that are offset toward lower equivalent widths of absorption.

I - **Strongly centrally peaking velocity dispersion profiles** are a property that appears to be exclusively that of classical bulges. Fabricius et al. (2012) finds that if a bulge has a logarithmic derivative that is more negative than $d\log(\sigma)/d\log(r) < -0.1$ the bulge is a classical bulge.

II- **Central Velocity Dispersion** of pseudobulges is systematically lower than that of classical bulges. If a bulge is found to have $\sigma_0 > 130 \text{ km s}^{-1}$ then that bulge is very likely to also show evidence of being a classical bulge, and is not likely a pseudobulge. However, a significant number of classical bulges have lower σ_0 than this.

The following criteria must be satisfied to be a defined, empirically as a classical bulge, but are not sufficient on their own to identify the bulge as a classical bulge.

III - Classical bulges are **Consistent with the Fundamental plane scaling relationships**.

III - **Low specific star formation rates and low central gas surface densities** are found in all classical bulges, that are not presently experiencing a merger. To be identified as a classical bulge we find that $SFR/M_* < 10^{-11} \text{ yr}^{-1}$ and $\Sigma_{mol} < 100 M_{\odot} \text{ pc}^{-1}$. Though many pseudobulge also have low star formation activity and likewise are gas poor, therefore an inactive ISM is not sufficient to identify a bulge as being either classical or pseudobulge.

III - **Classical bulges are not extremely blue**. There is no range in optical color that uniquely isolates classical bulges, however if a bulge is extremely blue it is not likely a classical bulge.

Acknowledgments DBF acknowledges support from Australian Research Council (ARC) Discovery Program (DP) grant DP130101460. We are grateful to D. Gadotti, and P. Erwin for making data and results available to us.

References

- Aguerri, J. A. L., Balcells, M., & Peletier, R. F. 2001, *A&A*, 367, 428
 Andredakis, Y. C., Peletier, R. F., & Balcells, M. 1995, *MNRAS*, 275, 874
 Andredakis, Y. C., & Sanders, R. H. 1994, *MNRAS*, 267, 283
 Athanassoula, E. 2005a, *MNRAS*, 358, 1477
 —. 2005b, *MNRAS*, 358, 1477
 Balcells, M., Graham, A. W., Domínguez-Palmero, L., & Peletier, R. F. 2003, *Ap.J Letters*, 582, L79
 Barth, A. J., Ho, L. C., & Sargent, W. L. W. 2002, *AJ*, 124, 2607
 Bender, R., Burstein, D., & Faber, S. M. 1992, *Ap.J*, 399, 462
 Blanton, M. R., Eisenstein, D., Hogg, D. W., Schlegel, D. J., & Brinkmann, J. 2005, *Ap.J*, 629, 143

- Böker, T., Laine, S., van der Marel, R. P., Sarzi, M., Rix, H.-W., Ho, L. C., & Shields, J. C. 2002, *AJ*, 123, 1389
- Boylan-Kolchin, M., Ma, C., & Quataert, E. 2006, *MNRAS*, 369, 1081
- Bruzual A., G. 1983, *Ap.J*, 273, 105
- Bundy, K., Bershad, M. A., Yan, R., Law, D., Drory, N., R., D., MacDonald, N., Wake, D. A., & Weijmans, A.-M. 2014, *ApJ*, submitted
- Bureau, M., & Freeman, K. C. 1999, *AJ*, 118, 126
- Buta, R., & Crocker, D. A. 1993, *AJ*, 105, 1344
- Buta, R. J., Corwin, H. G., & Odewahn, S. C. 2007, *The de Vaucouleurs Atlas of Galaxies* (Cambridge University Press)
- Calzetti, D., Kennicutt, R. C., Engelbracht, C. W., Leitherer, C., Draine, B. T., Kewley, L., Moustakas, J., Sosey, M., Dale, D. A., Gordon, K. D., Helou, G. X., Hollenbach, D. J., Armus, L., Bendo, G., Bot, C., Buckalew, B., Jarrett, T., Li, A., Meyer, M., Murphy, E. J., Prescott, M., Regan, M. W., Rieke, G. H., Roussel, H., Sheth, K., Smith, J. D. T., Thornley, M. D., & Walter, F. 2007, *Ap.J*, 666, 870
- Caon, N., Capaccioli, M., & D'Onofrio, M. 1994, *AAPs*, 106, 199
- Carollo, C. M. 1999, *Ap.J*, 523, 566
- Carollo, C. M., Stiavelli, M., de Zeeuw, P. T., & Mack, J. 1997, *AJ*, 114, 2366
- Carollo, C. M., Stiavelli, M., de Zeeuw, P. T., Seigar, M., & Dejonghe, H. 2001, *Ap.J*, 546, 216
- Comerón, S., Knapen, J. H., & Beckman, J. E. 2008, *A& A*, 485, 695
- Comerón, S., Knapen, J. H., Beckman, J. E., Laurikainen, E., Salo, H., Martínez-Valpuesta, I., & Buta, R. J. 2010, *MNRAS*, 402, 2462
- Cortese, L., Boselli, A., Franzetti, P., Decarli, R., Gavazzi, G., Boissier, S., & Buat, V. 2008, *MNRAS*, 386, 1157
- Courteau, S., de Jong, R. S., & Broeils, A. H. 1996, *Ap.J Letters*, 457, L73+
- Croom, S. M., Lawrence, J. S., Bland-Hawthorn, J., Bryant, J. J., Fogarty, L., Richards, S., Goodwin, M., Farrell, T., Miziarski, S., Heald, R., Jones, D. H., Lee, S., Colless, M., Brough, S., Hopkins, A. M., Bauer, A. E., Birchall, M. N., Ellis, S., Horton, A., Leon-Saval, S., Lewis, G., López-Sánchez, Á. R., Min, S.-S., Trinh, C., & Trowland, H. 2012, *MNRAS*, 421, 872
- de Jong, R. S. 1996, *A& A*, 313, 45
- de Vaucouleurs, G., de Vaucouleurs, A., Corwin, Jr., H. G., Buta, R. J., Paturel, G., & Fouque, P. 1991, *Third Reference Catalogue of Bright Galaxies (Volume 1-3, XII, 2069 pp. 7 figs.. Springer-Verlag Berlin Heidelberg New York)*
- Debattista, V. P., Carollo, C. M., Mayer, L., & Moore, B. 2004, *Ap.J Letters*, 604, L93
- Debattista, V. P., & Shen, J. 2007, *Ap.J Letters*, 654, L127
- Djorgovski, S., & Davis, M. 1987, *Ap.J*, 313, 59
- Draine, B. T., Aniano, G., Krause, O., Groves, B., Sandstrom, K., Braun, R., Leroy, A., Klaas, U., Linz, H., Rix, H.-W., Schinnerer, E., Schmiedeke, A., & Walter, F. 2014, *Ap.J*, 780, 172
- Drory, N., & Fisher, D. B. 2007, *Ap.J*, 664, 640
- Elmegreen, B. G., Bournaud, F., & Elmegreen, D. M. 2008, *Ap.J*, 688, 67

- Erwin, P. 2008, in IAU Symposium, Vol. 245, IAU Symposium, ed. M. Bureau, E. Athanassoula, & B. Barbuy, 113–116
- Erwin, P., Beckman, J. E., & Vega-Beltran, J.-C. 2004, in Astrophysics and Space Science Library, Vol. 319, Astrophysics and Space Science Library, ed. D. L. Block, I. Puerari, K. C. Freeman, R. Groess, & E. K. Block, 775–+
- Erwin, P., Saglia, R. P., Fabricius, M., Thomas, J., Nowak, N., Rusli, S., Bender, R., Vega Beltrán, J. C., & Beckman, J. E. 2015, MNRAS, 446, 4039
- Erwin, P., & Sparke, L. S. 2002, AJ, 124, 65
- Evans, II, N. J. 1999, ARA& A, 37, 311
- Faber, S. M., & Jackson, R. E. 1976, Ap.J, 204, 668
- Faber, S. M., Wegner, G., Burstein, D., Davies, R. L., Dressler, A., Lynden-Bell, D., & Terlevich, R. J. 1989, Ap.J Supplement, 69, 763
- Fabricius, M. H., Coccato, L., Bender, R., Drory, N., Gössl, C., Landriau, M., Saglia, R. P., Thomas, J., & Williams, M. J. 2014, MNRAS, 441, 2212
- Fabricius, M. H., Saglia, R. P., Fisher, D. B., Drory, N., Bender, R., & Hopp, U. 2012, Ap.J, 754, 67
- Falcón-Barroso, J., Bacon, R., Bureau, M., Cappellari, M., Davies, R. L., de Zeeuw, P. T., Emsellem, E., Fathi, K., Krajnović, D., Kuntschner, H., McDermid, R. M., Peletier, R. F., & Sarzi, M. 2006, MNRAS, 369, 529
- Falcón-Barroso, J., van de Ven, G., Peletier, R. F., Bureau, M., Jeong, H., Bacon, R., Cappellari, M., Davies, R. L., de Zeeuw, P. T., Emsellem, E., Krajnović, D., Kuntschner, H., McDermid, R. M., Sarzi, M., Shapiro, K. L., van den Bosch, R. C. E., van der Wolk, G., Weijmans, A., & Yi, S. 2011, MNRAS, 417, 1787
- Fernández Lorenzo, M., Sulentic, J., Verdes-Montenegro, L., Blasco-Herrera, J., Argudo-Fernández, M., Garrido, J., Ramírez-Moreta, P., Ruiz, J. E., Sánchez-Expósito, S., & Santander-Vela, J. D. 2014, Ap.J Letters, 788, L39
- Fisher, D. B. 2006, Ap.J Letters, 642, L17
- Fisher, D. B., Bolatto, A., Drory, N., Combes, F., Blitz, L., & Wong, T. 2013, Ap.J, 764, 174
- Fisher, D. B., & Drory, N. 2008, AJ, 136, 773
- . 2010, Ap.J, 716, 942
- . 2011, Ap.J Letters, 733, L47
- Fisher, D. B., Drory, N., & Fabricius, M. H. 2009, Ap.J, 697, 630
- Freeman, K. C. 1970, Ap.J, 160, 811
- Gadotti, D. A. 2008, MNRAS, 384, 420
- . 2009, MNRAS, 393, 1531
- . 2012, ArXiv e-prints
- Gadotti, D. A., & dos Anjos, S. 2001, AJ, 122, 1298
- Ganda, K., Peletier, R. F., McDermid, R. M., Falcón-Barroso, J., de Zeeuw, P. T., Bacon, R., Cappellari, M., Davies, R. L., Emsellem, E., Krajnović, D., Kuntschner, H., Sarzi, M., & van de Ven, G. 2007, MNRAS, 380, 506
- García-Burillo, S., Combes, F., & Neri, R. 1999, A& A, 343, 740
- Genzel, R., Burkert, A., Bouché, N., Cresci, G., Förster Schreiber, N. M., Shapley, A., Shapiro, K., Tacconi, L. J., Buschkamp, P., Cimatti, A., Daddi, E., Davies, R., Eisenhauer, F., Erb, D. K., Genel, S., Gerhard, O., Hicks, E., Lutz, D., Naab, T.,

- Ott, T., Rabien, S., Renzini, A., Steidel, C. C., Sternberg, A., & Lilly, S. J. 2008, *Ap.J*, 687, 59
- Graham, A., Lauer, T. R., Colless, M., & Postman, M. 1996, *Ap.J*, 465, 534
- Graham, A. W., & Driver, S. P. 2005, *Publications of the Astronomical Society of Australia*, 22, 118
- Hammer, F., Flores, H., Elbaz, D., Zheng, X. Z., Liang, Y. C., & Cesarsky, C. 2005, *A&A*, 430, 115
- Heller, C. H., Shlosman, I., & Athanassoula, E. 2007, *Ap.J Letters*, 657, L65
- Héraudeau, P., Simien, F., Maubon, G., & Prugniel, P. 1999, *AAPs*, 136, 509
- Inoue, S., & Saitoh, T. R. 2012, *MNRAS*, 2819
- Jogee, S., Scoville, N., & Kenney, J. D. P. 2005, *Ap.J*, 630, 837
- Kauffmann, G., Heckman, T. M., White, S. D. M., Charlot, S., Tremonti, C., Peng, E. W., Seibert, M., Brinkmann, J., Nichol, R. C., SubbaRao, M., & York, D. 2003, *MNRAS*, 341, 54
- Kautsch, S. J., Grebel, E. K., Barazza, F. D., & Gallagher, III, J. S. 2006, *A&A*, 445, 765
- Kenney, J. D. P., van Gorkom, J. H., & Vollmer, B. 2004, *AJ*, 127, 3361
- Kennicutt, R. C., & Evans, N. J. 2012, *ARA&A*, 50, 531
- Kennicutt, R. C., Hao, C., Calzetti, D., Moustakas, J., Dale, D. A., Bendo, G., Engelbracht, C. W., Johnson, B. D., & Lee, J. C. 2009, *Ap.J*, 703, 1672
- Kennicutt, Jr., R. C. 1998, *ARA&A*, 36, 189
- Khosroshahi, H. G., Wadadekar, Y., & Kembhavi, A. 2000, *Ap.J*, 533, 162
- Knapen, J. H. 2005, *A&A*, 429, 141
- Kormendy, J. 1977a, *Ap.J*, 218, 333
- . 1977b, *Ap.J*, 217, 406
- Kormendy, J. 1982, in *Saas-Fee Advanced Course 12: Morphology and Dynamics of Galaxies* Saas-Fee Vol. 12: Morphology and Dynamics of Galaxies, 113–288
- Kormendy, J. 1993, in *IAU Symp. 153: Galactic Bulges*, 209–+
- . 2013, *Secular Evolution in Disk Galaxies*, ed. J. Falcón-Barroso & J. H. Knapen, 1
- Kormendy, J., & Fisher, D. B. 2008, in *Astronomical Society of the Pacific Conference Series, Vol. 396*, *Astronomical Society of the Pacific Conference Series*, ed. J. G. Funes & E. M. Corsini, 297–+
- Kormendy, J., Fisher, D. B., Cornell, M. E., & Bender, R. 2009, *Ap.J Supplement*, 182, 216
- Kormendy, J., & Illingworth, G. 1982, *Ap.J*, 256, 460
- Kormendy, J., & Kennicutt, R. C. 2004, *ARA&A*, 42, 603
- Kuntschner, H., Emsellem, E., Bacon, R., Cappellari, M., Davies, R. L., de Zeeuw, P. T., Falcón-Barroso, J., Krajnović, D., McDermid, R. M., Peletier, R. F., Sarzi, M., Shapiro, K. L., van den Bosch, R. C. E., & van de Ven, G. 2010, *MNRAS*, 408, 97
- Lackner, C. N., & Gunn, J. E. 2012, *MNRAS*, 421, 2277
- Laurikainen, E., Salo, H., Buta, R., Knapen, J., Speltincox, T., & Block, D. 2006, *AJ*, 132, 2634

- Laurikainen, E., Salo, H., Buta, R., Knapen, J. H., & Comerón, S. 2010, *MNRAS*, 405, 1089
- Leroy, A. K., Bigiel, F., de Blok, W. J. G., Boissier, S., Bolatto, A., Brinks, E., Madore, B., Muñoz-Mateos, J.-C., Murphy, E., Sandstrom, K., Schruba, A., & Walter, F. 2012, *ArXiv e-prints*
- Lintott, C., Schawinski, K., Bamford, S., Slosar, A., Land, K., Thomas, D., Edmondson, E., Masters, K., Nichol, R. C., Raddick, M. J., Szalay, A., Andreescu, D., Murray, P., & Vandenberg, J. 2011, *MNRAS*, 410, 166
- MacArthur, L. A., Courteau, S., Bell, E., & Holtzman, J. A. 2004, *Ap.J Supplement*, 152, 175
- MacArthur, L. A., González, J. J., & Courteau, S. 2009, *MNRAS*, 395, 28
- Martig, M., Bournaud, F., Teyssier, R., & Dekel, A. 2009, *Ap.J*, 707, 250
- Möllenhoff, C. 2004, *A&A*, 415, 63
- Moorthy, B. K., & Holtzman, J. A. 2005, *astro-ph/0512346*
- Noguchi, M. 1999, *Ap.J*, 514, 77
- Obreja, A., Domínguez-Tenreiro, R., Brook, C., Martínez-Serrano, F. J., Doménech-Moral, M., Serna, A., Mollá, M., & Stinson, G. 2013, *Ap.J*, 763, 26
- Peletier, R. F. 2008, in *Astronomical Society of the Pacific Conference Series*, Vol. 390, *Pathways Through an Eclectic Universe*, ed. J. H. Knapen, T. J. Mahoney, & A. Vazdekis, 232
- Peletier, R. F., & Balcells, M. 1996, *AJ*, 111, 2238
- Peletier, R. F., Balcells, M., Davies, R. L., Andredakis, Y., Vazdekis, A., Burkert, A., & Prada, F. 1999, *MNRAS*, 310, 703
- Peletier, R. F., Falcón-Barroso, J., Bacon, R., Cappellari, M., Davies, R. L., de Zeeuw, P. T., Emsellem, E., Ganda, K., Krajnović, D., Kuntschner, H., McDermid, R. M., Sarzi, M., & van de Ven, G. 2007, *MNRAS*, 379, 445
- Proctor, R. N., & Sansom, A. E. 2002, *MNRAS*, 333, 517
- Regan, M. W., Thornley, M. D., Helfer, T. T., Sheth, K., Wong, T., Vogel, S. N., Blitz, L., & Bock, D. C.-J. 2001, *Ap.J*, 561, 218
- Renzini, A. 2006, *ARA&A*, 44, 141
- Robertson, B., Bullock, J. S., Cox, T. J., Di Matteo, T., Hernquist, L., Springel, V., & Yoshida, N. 2006, *Ap.J*, 645, 986
- Saglia, R. P., Fabricius, M., Bender, R., Montalto, M., Lee, C.-H., Riffeser, A., Seitz, S., Morganti, L., Gerhard, O., & Hopp, U. 2010, *A&A*, 509, A61
- Salim, S., Rich, R. M., Charlot, S., Brinchmann, J., Johnson, B. D., Schiminovich, D., Seibert, M., Mallery, R., Heckman, T. M., Forster, K., Friedman, P. G., Martin, D. C., Morrissey, P., Neff, S. G., Small, T., Wyder, T. K., Bianchi, L., Donas, J., Lee, Y.-W., Madore, B. F., Milliard, B., Szalay, A. S., Welsh, B. Y., & Yi, S. K. 2007, *Ap.J Supplement*, 173, 267
- Sandage, A. 1961, *The Hubble atlas of galaxies* (Washington: Carnegie Institution, 1961)
- Sandage, A., & Bedke, J. 1994, *The Carnegie atlas of galaxies* (Washington, DC: Carnegie Institution of Washington with The Flintridge Foundation, —c1994)
- Scarlata, C., Stiavelli, M., Hughes, M. A., Axon, D., Alonso-Herrero, A., Atkinson, J., Batcheldor, D., Binney, J., Capetti, A., Carollo, C. M., Dressel, L., Gerssen, J.,

- Macchetto, D., Maciejewski, W., Marconi, A., Merrifield, M., Ruiz, M., Sparks, W., Tsvetanov, Z., & van der Marel, R. P. 2004, *AJ*, 128, 1124
- Sérsic, J. L. 1968, *Atlas de galaxias australes* (Cordoba, Argentina: Observatorio Astronomico, 1968)
- Shen, J., & Debattista, V. P. 2009, *Ap.J*, 690, 758
- Sheth, K., Vogel, S. N., Regan, M. W., Thornley, M. D., & Teuben, P. J. 2005, *Ap.J*, 632, 217
- Smith, J. A., Tucker, D. L., Kent, S., Richmond, M. W., Fukugita, M., Ichikawa, T., Ichikawa, S.-i., Jorgensen, A. M., Uomoto, A., Gunn, J. E., Hamabe, M., Watanabe, M., Tolea, A., Henden, A., Annis, J., Pier, J. R., McKay, T. A., Brinkmann, J., Chen, B., Holtzman, J., Shimasaku, K., & York, D. G. 2002, *AJ*, 123, 2121
- Thomas, D., & Davies, R. L. 2006, *MNRAS*, 366, 510
- Weinzirl, T., Jogee, S., Khochfar, S., Burkert, A., & Kormendy, J. 2009, *Ap.J*, 696, 411
- Whitford, A. E. 1978, *Ap.J*, 226, 777
- Wyse, R. F. G., Gilmore, G., & Franx, M. 1997, *ARA& A*, 35, 637
- Young, L. M., Bureau, M., Davis, T. A., Combes, F., McDermid, R. M., Alatalo, K., Blitz, L., Bois, M., Bournaud, F., Cappellari, M., Davies, R. L., de Zeeuw, P. T., Emsellem, E., Khochfar, S., Krajnović, D., Kuntschner, H., Lablanche, P.-Y., Morganti, R., Naab, T., Oosterloo, T., Sarzi, M., Scott, N., Serra, P., & Weijmans, A.-M. 2011, *MNRAS*, 414, 940
- Zhao, Y. 2012, *Ap & SS*, 337, 719